

# The sudden approximation in photoemission and beyond

L. Hedin (1,2) and J. D. Lee (3)

1. *Dept. of Physics, University of Lund, Sölvegatan 14A, 22362 Lund, Sweden*

2. *MPI-FKF, Heisenbergstrasse 1, D-70569 Stuttgart, Germany*

3. *Dept. of Physics and Dept. of Complexity Science and Engineering, University of Tokyo, Bunkyo ku, Tokyo 113, Japan*

(June 11, 2018)

The conditions behind the sudden approximation are critically examined. The fuzzy band expression is derived in detail from first principles. We go beyond the sudden approximation to account for both extrinsic losses and interference effects. In an extension of earlier work we discuss both core and valence satellites including both intrinsic and extrinsic amplitudes, and high energy excitations as well as low energy electron-hole pairs. We show how the extrinsic losses in photoemission can be connected with the electron energy loss function. This is achieved by three approximations, to connect the dynamically screened potential in the bulk solid to the loss function, to account for the surface, and lastly to extrapolate zero momentum loss data to include dispersion. The extrinsic losses are found to be weak for small loss energies. For larger loss energies the extrinsic losses can be strong and have strong interference with the intrinsic losses depending on the nature of the solid. The transition from the adiabatic to the sudden regime is discussed for atoms and localized systems and compared with the situation for solids. We argue that in solids for photoelectron energies above some 10 eV the external losses are mainly connected with spatially extended excitations. We discuss strongly correlated quasi-two-dimensional solids with Bi2212 as example, and find an asymmetric broadening of the main peak from shake up of acoustic three-dimensional plasmons. In the superconducting state the loss function is assumed to have a gap, which then leads to a peak-dip-hump structure in the photoemission spectrum. This structure is compared with a corresponding structure in tunneling.

## I. INTRODUCTION

Photoemission spectroscopy (PES) has become an important tool to analyze electronic structure. The accuracy of the experimental energy resolution is now in the meV range, and sample control has reached a high level of reliability. Yet the theory used to interpret these high quality experimental results has great weaknesses. Often only the spectral function is compared to experiment. This means that e.g. the momentum dependence of the dipole matrix elements is neglected, as well as the extrinsic losses. Use of the spectral function is fine if we have well-defined sharp quasi-particle peaks, and want to do band structure mapping. As the experimental resolution increases and line shapes are resolved this level of approximation becomes increasingly doubtful. That is in particular true for strongly correlated systems like high temperature superconductors (HTC) which have important features that cannot be described by quasi-particle peaks.

Presently PES for HTC materials is often compared to spectral functions for models like the t-J one for a two-dimensional (2D) copper oxide layer. Such a model can only (at best) describe a narrow low energy region of the total excitation spectrum. The omitted degrees of freedom describe higher energies, and also collective low energy modes with three-dimensional character. As far as we know, there has been no systematic attempt to develop a theory that both gives a good description of the

strongly correlated system and also takes account of the remaining correlations. This is an important and urgent problem if we want to have a true a priori understanding of e.g. HTC materials. In lack of a systematic theory we sketch below an approach to this problem built on physical intuition.

The 2D problem is normally treated with a model Hamiltonian based on a small number of orbitals  $\{\phi_{2D}\}$ . The parameters in the model Hamiltonian can be obtained from "down-folding" the basis functions in a band-structure calculation by using e.g. developments of the very efficient LMTO formalism [1]. The interesting correlation effects come from the degeneracy in the problem, i.e. the large number of possibilities to occupy the different  $m_l$  and  $m_s$  states of the localized muffin tin orbitals connected with the down-folded part of the band-structure. There are also efficient methods based on the LMTO formalism to handle a wide energy range which treats valence and conduction bands on an equal footing so that the wave functions are orthogonal [2]. Let's call the additional set of states beyond  $\{\phi_{2D}\}$  for  $\{\phi_{3D}\}$ . We assume that  $\{\phi_{3D}\}$  is strictly orthogonal to  $\{\phi_{2D}\}$  despite any complications that can come from down-folding. The one electron states  $\{\phi_{2D}\}$  give rise to a huge number of configurations which then all are orthogonal to the configurations that can be built from the set  $\{\phi_{3D}\}$ . We also assume that we can write the state vectors as a direct product,  $|\Psi_{tot, s_1, s_2}\rangle = |\Psi_{2D, s_1}\rangle |\Psi_{3D}^{(s_1)}, s_2\rangle$ , where

both the 2D and 3D parts are correlated state vectors. A parametric dependence of the 3D state on the 2D state is obvious when we have a core hole in the 2D system, but is actually important also in general.

When we develop our theory we will not make any specific assumptions about the correlations in the 2D system. We will assume that the excitations in the 3D system are extended in space and can be described by a quasi-boson model. This is possible if we only want to describe PES for energies larger than about 10 eV where a strongly correlated localized system already has reached the sudden limit. [3] The treatment here of strongly correlated systems is based on our recent work. [4]

## II. THE "ONE-STEP" THEORY

Bandstructure and surface effects in photoemission are today often treated in the so called "one-step model" pioneered by Pendry [5], [6], for recent reviews see e. g. Refs. [7], [8], [9], [10]. In the one-step model the important dipole matrix elements are included, as well as surface photoemission (emission due to the gradient in the electromagnetic field, for recent work see e. g. Ref. [11]), but not the extrinsic losses.

A complete theory was developed by Caroli et al in 1973 [12] based on the three current expression of Schaich and Ashcroft. [13] The Caroli et al theory uses the Keldysh formalism [14] for non-equilibrium Green's functions. It is exact and one can e.g. identify the diagrams which give extrinsic losses. Caroli et al did not however extract any practical calculation scheme from their theory.

Important steps towards a practical photoemission theory were taken by Feibelman and Eastman [15] and by Pendry [5], [6], who discussed the lowest non-trivial diagram in the Caroli et al expansion, assuming the final states to be (time-inverted) LEED scattering states. Pendry and collaborators developed an explicit multiple scattering formulation and computer programs rooted in earlier work on the LEED problem. [16] A careful discussion of the Caroli et al theory and the basics of photoemission was given by Almladh 1985 leading to some explicit approximations. [17]

With today's precise experimental data on photoemission the need for a comprehensive and practical theory is great. The one-step theory has serious limitations both in its theoretical foundation and in its scope. Thus Pendry, Feibelman and Eastman just assumed that the photoelectron states should be damped. That this is correct was shown later by Almladh, however he uses the Keldysh diagram expansion which is rather involved. More serious is that the one-step theory neglects the extrinsic losses. These losses were early recognized to be important, and in core electron photoemission they are routinely included. That they also are important in photoemission from an extended state (valence electrons) is not

as widely recognized.

A full theory for photoemission has a number of intriguing features. We will display some of them by starting from the Golden Rule expression rather than the Keldysh expansion, and postulating a simple model Hamiltonian. Exact results can then be obtained by elementary means. The model Hamiltonian will be motivated a posteriori by discussing cases where the results can be obtained by other means.

The Golden Rule expression for the photo-electron current can be obtained from scattering theory [18] (we use atomic units,  $e = \hbar = m = 1$ , and thus e.g. energies are in Hartrees, 27.2 eV),

$$J_{\mathbf{k}}(\omega) = \sum_s |\langle N-1, s; \mathbf{k} | \Delta | N \rangle|^2 \delta(\omega - \varepsilon_{\mathbf{k}} + \varepsilon_s). \quad (1)$$

The final states  $|N-1, s; \mathbf{k}\rangle$  have the proper boundary conditions for scattering states. All states are correlated. Further  $\varepsilon_{\mathbf{k}}$  is the energy of the photo-electron,  $\varepsilon_{\mathbf{k}} = \mathbf{k}^2/2$  [19],  $\varepsilon_s$  gives the energy of the final state of the solid as  $\varepsilon_s = E(N, 0) - E(N-1, s)$ ,  $\omega$  is the photon energy, and  $\Delta$  the optical transition operator,

$$\Delta = \sum_{ij} \Delta_{ij} c_i^\dagger c_j, \quad \Delta_{ij} = \langle i | Ap + pA | j \rangle.$$

$|N\rangle$  is the initial state. The exact expression for  $J_{\mathbf{k}}(\omega)$  is rather intractable, and we have to develop approximations that can be handled. [20], [21], [22] For non-interacting electrons where  $|N-1, s; \mathbf{k}\rangle$  and  $|N\rangle$  are Slater determinants, it is easy to see that  $|N-1, s; \mathbf{k}\rangle = c_{\mathbf{k}}^\dagger c_s |N\rangle$ , and thus Eq. 1 reduces to the well-known form

$$J_{\mathbf{k}}(\omega) = \sum_s^{occ} |\Delta_{\mathbf{k}s}|^2 \delta(\omega - \varepsilon_{\mathbf{k}} + \varepsilon_s),$$

where the index "s" now stands for an occupied one-electron state (e.g. a core electron state or a state in the valence band).

The final state can be written as,

$$|N-1, s; \mathbf{k}\rangle = \left[ 1 + \frac{1}{E - H - i\eta} (H - E) \right] c_{\mathbf{k}}^\dagger |N-1, s\rangle, \quad (2)$$

where  $H$  is the fully interacting Hamiltonian including target electrons and photoelectron, and  $E = \omega + E(N, 0) = \varepsilon_{\mathbf{k}} + E(N-1, s)$ . Further  $|N-1, s\rangle$  is the target state after the photo-electron has left, and  $c_{\mathbf{k}}^\dagger$  creates the photoelectron. The states corresponding to  $c_{\mathbf{k}}^\dagger$  are so far undefined, except that they are time-inverted LEED states with asymptotically a plane wave part  $\exp(i\mathbf{k} \cdot \mathbf{r})$ . Usually in scattering problems  $(H - E)$  is replaced by the interaction  $V$  between the scattering particle and the target. This is not possible when the scattering particle is identical with particles in the target. One way to avoid this difficulty is to regard the scattering particle as different, and do an anti-symmetrization

of the solution at the end of the analysis, which is the route followed in the standard treatise of scattering by Goldberger and Watson. [18]

At high energies we can regard the scattering particle as different from the particles in the target since the exchange coupling becomes negligible. We can then replace  $(H - E)$  by a potential  $V$  which describes the coupling between the photoelectron and the density fluctuations in the solid. [21] This is true for all systems, also strongly correlated ones. For strongly correlated *localized* systems the interaction with the photoelectron becomes small already at energies of about 10 eV. [3] As discussed in the introduction we will take the total wave function as a direct product,  $|\Psi_{tot}, s_1, s_2\rangle = |\Psi_{2D}, s_1\rangle |\Psi_{3D}^{(s_1)}, s_2\rangle$ . For energies above 10 eV we only need to consider the interaction between the photoelectron and the excitations "s<sub>2</sub>".

If the  $(H - E)$  term, which gives the extrinsic scattering, is neglected, and if we assume that  $c_{\mathbf{k}}|N\rangle = 0$ , the amplitude becomes

$$\langle N - 1, s; \mathbf{k} | \Delta | N \rangle = \sum_j \langle \mathbf{k} | \Delta | j \rangle \langle N - 1, s | c_j | N \rangle. \quad (3)$$

The photo current in Eq. 1 is then given by the spectral function  $A_{ij}(\varepsilon_{\mathbf{k}} - \omega)$ ,

$$J_{\mathbf{k}}(\omega) = \sum_{ij} \langle \mathbf{k} | \Delta | i \rangle A_{ij}(\varepsilon_{\mathbf{k}} - \omega) \langle j | \Delta | \mathbf{k} \rangle, \quad (4)$$

where

$$A_{ij}(\omega) = \sum_s^{\varepsilon_s < \mu} \langle N | c_i^\dagger | N - 1, s \rangle \langle N - 1, s | c_j | N \rangle \times \delta(\omega - \varepsilon_s). \quad (5)$$

Eq. 4 is the well-known intrinsic approximation for the photocurrent. The photoelectron states  $|\mathbf{k}\rangle$  are time-inverted LEED states (with no magnetic field this just means complex conjugation). A LEED state has an incoming and a set of scattered plane waves outside the solid, matched to a solution inside the solid with a potential  $V_H + \Sigma(\varepsilon_{\mathbf{k}})$ , where  $V_H(\mathbf{r})$  is the Hartree potential for a finite solid with a surface and  $\Sigma$  the complex selfenergy. In the next section we will show how the perturbation  $V$  gives rise to extrinsic energy losses and the selfenergy term  $\Sigma(\varepsilon_{\mathbf{k}})$ .

In the one-electron approximation the spectral function is diagonal and has just one quasi-particle peak,  $A_{ij}(\omega) = \delta(\omega - E_i) \delta_{ij}$ . In most applications the spectral function is taken as diagonal. This is e.g. generally justified in the GW approximation. [22] A core electron spectral function for a metal  $A_c(\omega)$  has an asymmetric peak (MND singularity [23]) followed by a set of plasmon peaks. The asymmetry is due to shake-up of electron-hole pairs and phonons. [24] For a conduction electron in a metal the spectral function  $A_{\mathbf{k}}(\omega)$  looks quite similar with a broadened and asymmetric quasi-particle peak

and a pronounced satellite structure. The broadening and asymmetry however go to zero at the Fermi level. Semiconductors have no low energy electron-hole excitations and thus lack the MND singularity, but still have pronounced plasmon satellites. Transition metals have about the same total strength in the satellite structure, but lack the pronounced high energy peaks of sp-metals and valence semiconductors. Strongly correlated materials may lack the quasi-particle peak altogether, and have all the spectral strength in the satellite.

For core electron photoemission the current in the intrinsic approximation is simply  $J_{\mathbf{k}}(\omega) = |\langle \mathbf{k} | \Delta | c \rangle|^2 A_c(\varepsilon_{\mathbf{k}} - \omega)$ . For valence electrons we need a more involved discussion. We denote the initial state "j" in Eq. 3 with a vector  $\mathbf{l}$  which also includes a bandindex, and Eq. 4 becomes

$$J_{\mathbf{k}}(\omega) = \sum_{\mathbf{l}} |\langle \mathbf{k} | \Delta | \mathbf{l} \rangle|^2 A_{\mathbf{l}}(\varepsilon_{\mathbf{k}} - \omega). \quad (6)$$

For energies close to the quasi-particle energy  $E_{\mathbf{l}}$ , the spectral function  $A_{\mathbf{l}}$  has the form (neglecting the asymmetry, which can be pronounced away from the Fermi level)

$$A_{\mathbf{l}}(\omega) = \frac{Z_{\mathbf{l}}}{\pi} \frac{\Gamma_{\mathbf{l}}}{(\omega - E_{\mathbf{l}})^2 + \Gamma_{\mathbf{l}}^2}, \quad (7)$$

which together with Eq. 6 gives the one-step approximation. The photoelectron wavefunction  $|\mathbf{k}\rangle$  inside the solid is determined by the potential  $V_H(\mathbf{r}) + \Sigma(\mathbf{r}, \mathbf{r}'; \varepsilon_{\mathbf{k}})$ , where  $V_H$  is the Hartree or Coulomb potential. The real part of the non-local optical potential or selfenergy  $\Sigma$  is usually approximated by a local potential and combined with  $V_H$  to give an effective potential  $V_{eff}$ . Replacing  $-\text{Im} \Sigma$  by its expectation value  $\Gamma_f > 0$ , and setting  $|\mathbf{k}\rangle = |\tilde{\mathbf{k}}\rangle$  inside the solid, we have

$$(t + V_{eff} - i\Gamma_f) |\tilde{\mathbf{k}}\rangle = \varepsilon_{\mathbf{k}} |\tilde{\mathbf{k}}\rangle, \quad (8)$$

where  $t$  is the kinetic energy,  $\Gamma_f = -\langle \tilde{\mathbf{k}} | \text{Im} \Sigma(\varepsilon_{\mathbf{k}}) | \tilde{\mathbf{k}} \rangle > 0$  and  $\varepsilon_{\mathbf{k}} = \mathbf{k}^2/2$ . The photoelectron wavefunction  $|\tilde{\mathbf{k}}\rangle$  inside the solid can be written as a combination of Bloch functions with complex  $\mathbf{k}$  vectors, such that it correctly matches the plane waves outside the solid. If one Bloch wave dominates [25] its complex momentum  $\tilde{\mathbf{k}}$  follows from

$$E_{\tilde{\mathbf{k}}} = \varepsilon_{\mathbf{k}} + i\Gamma_f,$$

where  $E_{\tilde{\mathbf{k}}}$  is the complex quasiparticle energy having both a shift in its real part from  $\text{Re} \Sigma$  and an imaginary part  $\Gamma_f$ . We write  $\tilde{\mathbf{k}} = \tilde{\mathbf{k}}_{\parallel} + \hat{z}(\tilde{k}_z + ik_f^I)$ , where  $\tilde{\mathbf{k}}_{\parallel}$  is parallel to the surface and  $\hat{z}$  is a unit vector normal to the surface. Due to momentum conservation we have  $\tilde{\mathbf{k}}_{\parallel} = \mathbf{k}_{\parallel}$ .

In the limit of small  $\Gamma_f$  we can expand  $E_{\tilde{\mathbf{k}}} = E_{\text{Re}\tilde{\mathbf{k}}} + i \text{Im}\tilde{\mathbf{k}} \partial E_{\tilde{\mathbf{k}}}/\partial \tilde{\mathbf{k}}$ , and thus we have

$$k_f^I = \frac{\Gamma_f}{\partial E_{\tilde{\mathbf{k}}}/\partial k_z}.$$

Mahan [26] and in more detail Spanjaard et al [25] studied the matrix element  $\langle \tilde{\mathbf{k}}|\Delta|\mathbf{1}\rangle$  in the limit when the damping is small. The integration parallel to the surface gives momentum conservation,  $\tilde{\mathbf{k}}_{\parallel} = \mathbf{1}_{\parallel}$ . The integration in the  $z$  direction gives a surface contribution plus contributions from the unit cells where there is bulk symmetry. With bulk symmetry all cells give the same contribution but for a factor, and we can sum to have

$$\begin{aligned} & \langle \tilde{\mathbf{k}}|\Delta|\mathbf{1}\rangle \\ &= \left\{ \langle \tilde{\mathbf{k}}|\Delta|\mathbf{1}\rangle_{surf} + \frac{\langle \tilde{\mathbf{k}}|\Delta|\mathbf{1}\rangle_0}{1 - \exp\left[i(l_z - \tilde{k}_z)c - k_f^I c\right]} \right\} \delta_{\tilde{\mathbf{k}}_{\parallel}, \mathbf{1}_{\parallel}}, \end{aligned} \quad (9)$$

where  $c$  is the cell length in the  $z$  direction and  $\langle \tilde{\mathbf{k}}|\Delta|\mathbf{1}\rangle_0$  is the integral over the first (closest to the surface) bulk unit cell. Band indices and 2D reciprocal lattice vectors have to be supplemented where appropriate. With small  $k_f^I$  and neglecting the surface contribution  $|\langle \tilde{\mathbf{k}}|\Delta|\mathbf{1}\rangle|^2$  is sharply peaked as function of  $l_z$  around  $l_z^0$ ,

$$l_z^0 = \text{mod}(\tilde{k}_z, 2\pi/c),$$

and one can approximate

$$|\langle \tilde{\mathbf{k}}|\Delta|\mathbf{1}\rangle|^2 = \frac{1}{c^2} \frac{|\langle \tilde{\mathbf{k}}|\Delta|\mathbf{1}^0\rangle_0|^2}{(l_z^0 - l_z)^2 + (k_f^I)^2} \delta_{\tilde{\mathbf{k}}_{\parallel}, \mathbf{1}_{\parallel}},$$

where  $|\mathbf{1}^0\rangle$  is a wavefunction in the occupied valence band, and

$$\mathbf{1}^0 = \mathbf{k}_{\parallel} + \hat{z}l_z^0 = \mathbf{1}^0(\mathbf{k}).$$

The surface contribution to the photocurrent can be comparable to the bulk one, and interference between the two terms in Eq. 9 is then important. [11], [27] Collecting our results the contribution to the photocurrent from the quasi-particle peak is

$$\begin{aligned} & J_{\mathbf{k}}(\omega) \\ &= \sum_{\mathbf{1}} \delta_{\tilde{\mathbf{k}}_{\parallel}, \mathbf{1}_{\parallel}} \frac{Z_1}{\pi c^2} \frac{\Gamma_i}{(\varepsilon_{\mathbf{k}} - E_1 - \omega)^2 + \Gamma_i^2} \frac{|\langle \tilde{\mathbf{k}}|\Delta|\mathbf{1}^0\rangle_0|^2}{(l_z^0 - l_z)^2 + (k_f^I)^2}, \end{aligned}$$

where  $\Gamma_i = \Gamma_1$ .

With  $\Gamma_i$  small we can expand  $\varepsilon_{\mathbf{k}} - E_1 - \omega = -(l_z - l_z^1) \partial E_1/\partial l_z$ , where  $l_z^1$  is given by the resonance condition

$$\varepsilon_{\mathbf{k}} - E_{\mathbf{k}_{\parallel} + \hat{z}l_z^1} - \omega = 0. \quad (10)$$

We define

$$\mathbf{1}^1 = \mathbf{k}_{\parallel} + \hat{z}l_z^1 = \mathbf{1}^1(\mathbf{k}, \omega).$$

When also  $\Gamma_i$  is small we can integrate over  $l_z$  keeping everything constant except the resonance denominators. We then have a convolution of two Lorentzians, which gives a new Lorentzian with the sum of the widths

$$\begin{aligned} & J_{\mathbf{k}}(\omega) \\ & \sim \left( \frac{1}{k_i^I} + \frac{1}{k_f^I} \right) \left| \frac{\partial E_1}{\partial l_z} \right|^{-2} \frac{1}{c^2} \frac{Z_1 \Gamma_i |\langle \tilde{\mathbf{k}}|\Delta|\mathbf{1}^0\rangle_0|^2}{(l_z^0 - l_z^1)^2 + (k_i^I + k_f^I)^2}, \end{aligned} \quad (11)$$

where

$$k_i^I = \left( \frac{\Gamma_i}{\partial E_1/\partial l_z} \right)_{l_z=l_z^0}, \quad k_f^I = \left( \frac{\Gamma_f}{\partial E_{\mathbf{k}}/\partial k_z} \right)_{\mathbf{k}=\text{Re}\tilde{\mathbf{k}}}.$$

The momentum parallel to the surface is conserved,  $\tilde{\mathbf{k}}_{\parallel} = \mathbf{k}_{\parallel}$ , and thus immediately follows from experiment while the determination of  $\tilde{k}_z$  requires knowledge of  $V_{eff}$  and thus e.g.  $\text{Re}\Sigma$ . There are however more involved experimental techniques to obtain also  $\tilde{k}_z$ . [28] As before band indices and 2D reciprocal lattice vectors have to be supplemented where appropriate.

The transmission problem related to the matching of the photoelectron wavefunction inside the solid and the plane waves outside has been studied by Spanjaard et al. [25] who conclude that for Ag the transmission factor is about 0.5 at all angles and for all energies of interest. The connection of the "fuzzy band" expression and different modes of experiment has been discussed in detail by Smith et al. [29] The deviation from free electron energies for the higher bands, which shows up as the difference between  $\tilde{\mathbf{k}}$  and  $\mathbf{k}$ , persist quite high up in energy. [30]

### III. EXTRINSIC LOSSES AND THE SUDDEN APPROXIMATION

The importance of extrinsic losses was recognized early, and the landmark paper here is the discussion by Berglund and Spicer in 1964 of the "three step model". [31] The three steps are photoexcitation, transport to the surface, and passage through the surface. In the last two steps the electrons can loose energy (extrinsic losses). Core electron photoemission data are often analyzed taking extrinsic losses into account. Methods to do this have been developed in a long series of papers by Tougaard and collaborators [32]. Strong extrinsic losses also occur in valence electron spectra. In Fig. 1 we show

the XPS valence band spectrum from Na metal found by Höchst, Steiner and Hüfner [33]. More details can be found in Refs. [34], [35]. It is remarkable that the structure from the plasmon satellites is as strong as the main band (first peak). Actually the valence electron spectrum is similar to the core electron spectrum. This similarity is very close, the full drawn line in Fig. 1 is obtained by convoluting the Na core spectrum with a valence band spectrum obtained by weighing the partial densities of states (shown in the inset) with coefficients used as free parameters (s:p:d=1:5:9). This picture is confirmed by theoretical work. [36], [37]

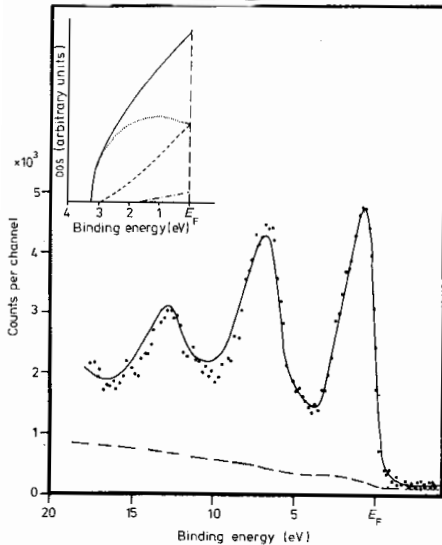


FIG. 1. XPS valence band spectrum of Na metal. Points are the experimental data and the full curve is the generated spectrum. The broken curve is the fitted background. The inset shows the total and partial densities of states (DOS) which were used to obtain the generated spectrum. Full curve, total DOS; dotted curve, *s* partial DOS; broken curve, *p* partial DOS; chain curve, *d* partial DOS.[33]

The plasmon satellites in the core spectrum are easy to understand, the sudden creation of a core hole changes the potential on the valence electrons and we have a "shake-up" effect. The surprising fact is that the sudden removal of a valence electron has a very similar shake-up effect, it is as if the valence electron hole were localized. A quantitative analysis of core electron satellites showed that both extrinsic and intrinsic losses contributed comparable amounts. [38] Since the valence satellites could be reproduced using the core spectra, we expect that also for valence electrons both intrinsic and extrinsic losses will contribute.

A theoretical analysis of satellites in simple metals was done by Penn both for core spectra, [39] and valence spectra, [36]. He solved a transport equation with the spectral function as source term. The spectral function for core electrons had been obtained by Langreth. [40] For valence

electrons Penn obtained a spectral function quite similar to the core one by doing lowest order perturbation theory using an effective Hamiltonian based on the Bohm-Pines plasmon theory. Penn's result clearly demonstrated that both intrinsic and extrinsic effects contributed to the satellites.

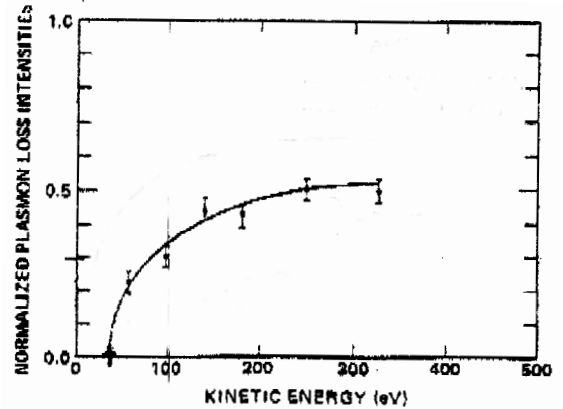


FIG. 2. Intensity of the first bulk plasmon satellite relative to the main peak for the *Al 2p* core electron spectrum. [45]

As analyzed by Chang and Langreth [41], [42] there must be interference between the intrinsic and extrinsic processes since they lead to the same final state for the system. In particular they discussed "sp-solids" and found the interference effects to be strong and fade off only at kinetic energies in the keV region. A detailed and quantitative theory of interference effects in a core electron spectrum was developed by Inglesfield using electron-plasmon coupling functions. [43], [44] Experimental results for the onset of the first plasmon satellite as function of kinetic energy have been obtained by Flodström et al. [45] (see Fig. 2), and of others (see e. g. Ref. [35]). Their results are well reproduced by Inglesfield's theory. [44]

A more general approach based on a quasi-boson model, fluctuation potentials and the GW approximation was developed by Hedin and collaborators. [46], [20], [37], [22] These results also show that both extrinsic and intrinsic effects are important, and that interference persists in simple metals to quite high kinetic energies. This approach has a more rigorous basis and should be quantitatively more reliable. In particular it handles not only plasmon losses but also the low energy electron-hole losses which lead to the Mahan-Nozieres-deDominicis (MND) singular threshold behavior. [23] We will now discuss photoemission using this quasi-boson model.

Following earlier work by Hedin et al [20], [21], [22] we use a quasi-boson model Hamiltonian,

$$H = H_0 + V, \quad H_0 = H_{syst} + h, \quad (12)$$

where

$$H_{syst} = \sum_l \varepsilon_l c_l^\dagger c_l + \sum_q \omega_q a_q^\dagger a_q + \sum_{ql'} V_{ll'}^q c_l^\dagger c_{l'} [a_q + a_q^\dagger],$$

$$h = \sum_{\mathbf{k}} \varepsilon_{\mathbf{k}} c_{\mathbf{k}}^\dagger c_{\mathbf{k}}, \quad V = \sum_q V^q [a_q + a_q^\dagger], \quad V^q = \sum_{\mathbf{k}\mathbf{k}'} V_{\mathbf{k}\mathbf{k}'}^q c_{\mathbf{k}}^\dagger c_{\mathbf{k}'}$$

Here indices "l" label states below and "k" states above the Fermi level. Thus "l" can stand for a core electron state or an occupied Bloch state in the valence band, and "k" is a state above the Fermi level (but possibly below the vacuum level). States below the vacuum level (occupied and unoccupied) are modified by the presence of the surface and have exponentially decaying amplitudes outside the solid. States above the vacuum level have the photoelectron boundary condition, i.e. they are time-inverted electron scattering states (LEED states) with free electron energies,  $\varepsilon_{\mathbf{k}} = \mathbf{k}^2/2$  and are plane waves at large distances from the solid. As basis set for the one-electron wavefunctions we take the eigenfunctions of the Hartree-Fock Hamiltonian. [22] We will suppress spin variables. The term  $V$  describes the interaction between the photoelectron and charge density fluctuations (see below) in the solid, i.e. it is the interaction which causes the extrinsic losses and also the damping of the photoelectrons. Further  $a_q$  stands for quasi-boson type excitations like electron-hole pairs, plasmons etc., and  $\omega_q$  is the quasi-boson energy. The quasi-boson parameters are related to the dynamically screened potential  $W(\mathbf{r}, \mathbf{r}'; \omega)$  as described in Appendix A. The potentials  $V^q(\mathbf{r})$  and the wavefunctions can be chosen to be real functions, which we use in the derivations. The final expressions are valid also with complex functions.

The model Hamiltonian we have defined clearly can only give an approximate description of a real system. Thus we obviously do some double counting of the Coulomb interactions. Despite this the predictions from the model Hamiltonian are basically sound. For self-energies it correctly describes the GW approximation, and it gives realistic results for both intrinsic and extrinsic effects in core electron photoemission. [22] The intrinsic satellites in valence electron photoemission for simple metals come out qualitatively correctly. [37] Further the high energy limit in photoemission is correctly described. [21] Clearly a quasi-boson model cannot handle strongly correlated systems, and we will discuss these separately.

Returning to Eq. 2 we take  $|N-1, s\rangle$  as an eigenfunction of  $H_{syst}$  with eigenvalues  $\omega_s$ , and thus  $c_{\mathbf{k}}^\dagger |N-1, s\rangle$  is an eigenfunction of  $H_0$  with eigenvalue  $\varepsilon_{\mathbf{k}} + \omega_s$ . Since  $E = \varepsilon_{\mathbf{k}} + \omega_s$  we can replace  $(H - E)$  with  $V$ . The states  $|N-1, s\rangle$  have a hole after the emitted photoelectron plus a number of boson type excitations. For core electron photoemission the bosons have to be calculated in a potential with a core hole present, while the initial state  $|N\rangle$  is the vacuum state of bosons with no core hole. Also in valence electron photoemission, as we have discussed earlier, the hole after the valence electron has a strong effect on the quasi-bosons leading to a comparable strength in the satellite.

For the photoemission amplitude we now have (suppressing the strongly correlated part in the problem),

$$\begin{aligned} & \langle N-1, s; \mathbf{k} | \Delta | N \rangle \\ &= \sum_{ij} \Delta_{ij} \left\langle N-1, s \left| c_{\mathbf{k}} \left[ 1 + V \frac{1}{E - H + i\eta} \right] c_i^\dagger c_j \right| N \right\rangle. \end{aligned} \quad (13)$$

The physical significance of this expression is quite clear. The operator  $c_i^\dagger c_j$  lifts one electron from the state "j" into the state "i". The "virtual" electron "i" propagates by  $(E - H)^{-1}$  and is then scattered by  $V$  into the state "k" which is measured by the detector. The state "i" must be a photoelectron state, which we denote by  $|\mathbf{k}'\rangle$ . Since we never have more than one photoelectron we can work with a product representation,

$$c_{\mathbf{k}}^\dagger |N-1, s\rangle = |N-1, s\rangle |\mathbf{k}\rangle, \quad c_{\mathbf{k}'}^\dagger |N\rangle = |N\rangle |\mathbf{k}'\rangle.$$

We can now rewrite Eq. 13 as

$$\begin{aligned} & \langle N-1, s; \mathbf{k} | \Delta | N \rangle \\ &= \sum_{j\mathbf{k}'} \left\langle \mathbf{k} \left| \left\langle N-1, s \left[ 1 + V \frac{1}{E - H + i\eta} \right] c_j \right| N \right\rangle \right| \mathbf{k}' \rangle \\ & \quad \times \langle \mathbf{k}' | \Delta | j \rangle \\ &= \sum_j \left\langle \mathbf{k} \left| \left\langle N-1, s \left[ 1 + V \frac{1}{E - H + i\eta} \right] c_j \right| N \right\rangle \Delta \right| j \rangle, \end{aligned} \quad (14)$$

noting that  $\sum_{\mathbf{k}'} |\mathbf{k}'\rangle \langle \mathbf{k}'|$  acts as a deltafunction.

The potential  $V$  in Eq. 14 gives the two effects of a loss potential, the energy loss scattering and the related reduction in the intensity of the no-loss peak. The latter comes through a partial summation over the no-loss intermediate state, which gives a damped photoemission wavefunction. Formally this summation can be done by use of the Feshbach projection operator technique. The result is (see e.g. Ref. [21])

$$\begin{aligned} & \langle N-1, s; \mathbf{k} | \Delta | N \rangle = \\ & \sum_j \left\langle \tilde{\mathbf{k}} \left| \left\langle N-1, s \left[ 1 + V \frac{1}{E - QHQ + i\eta} \right] c_j \right| N \right\rangle \Delta \right| j \rangle, \end{aligned} \quad (15)$$

where  $|\tilde{\mathbf{k}}\rangle$  is the wavefunction discussed in connection with Eq. 8, and  $Q$  is the projection operator  $Q = 1 - P$ , with  $P = |N-1, s\rangle \langle N-1, s|$ . In principle  $|\tilde{\mathbf{k}}\rangle$  and the self-energy,

$$\Sigma = PVQ \frac{1}{E - QHQ + i\eta} QVP,$$

depend on the excitation state of the target, "s". To lowest order we have [47]

$$\Sigma(\mathbf{r}, \mathbf{r}'; \omega) = \sum_q V^q(\mathbf{r}) \frac{1}{\omega - h - \omega_q + i\eta} V^q(\mathbf{r}'), \quad (16)$$

provided the quasi-bosons in the state "s" are extended and thus a finite number of them have a negligible influence. Also when we go to higher orders the result remains independent on the index "s". The imaginary part of  $\Sigma$  in Eq. 16 agrees with the imaginary part in the GW approximation for the self-energy [47], while the real parts differ slightly.

To estimate the extrinsic and intrinsic losses we expand Eq. 15 to lowest non-trivial order in  $V^q$  (see Appendix B). To lowest order in  $V$  there is one contribution from  $V(E - H_0)^{-1}$  (extrinsic loss) and one from  $\langle N - 1, s | c_j | N \rangle$  (intrinsic loss described by the spectral function). In both cases "s" is a state with one quasi-boson ( $q$ ) and one hole. The result is given in Eqs. 42 and 43. The selfenergy  $\Sigma$  in the denominator does not appear in the simplest lowest order perturbation theory but is obtained in a systematic expansion. [20], [47]

We first discuss valence electron photoemission when the index  $l$  is a vector index  $\mathbf{l}$ . From the discussion at the end of Sect II we see that the matrix element  $\langle \tilde{\mathbf{k}} | \Delta | \mathbf{l} \rangle$  is peaked around  $\mathbf{l} = \mathbf{l}^0$ . The no-loss contribution to  $J_{\mathbf{k}}(\omega)$  is

$$\begin{aligned} J_{\mathbf{k}}^0(\omega) &= \sum_{\mathbf{l}} \left| \langle \tilde{\mathbf{k}} | \Delta | \mathbf{l} \rangle \right|^2 \delta(\omega - \varepsilon_{\mathbf{k}} + \varepsilon_{\mathbf{l}}) \\ &= \frac{1}{c^2} \int \frac{\left| \langle \tilde{\mathbf{k}} | \Delta | \mathbf{l}^0 \rangle_0 \right|^2}{(l_z^0 - l_z)^2 + (k_f^l)^2} \delta(\omega - \varepsilon_{\mathbf{k}} + \varepsilon_{\mathbf{l}}) dl_z \\ &= \frac{1}{c^2} \frac{1}{|\partial \varepsilon_{\mathbf{l}} / \partial l_z|} \frac{\left| \langle \tilde{\mathbf{k}} | \Delta | \mathbf{l}^0 \rangle_0 \right|^2}{(l_z^0 - l_z^1)^2 + (k_f^l)^2}, \end{aligned}$$

which is the QP particle result in Eq. 11 in the limit when  $\Gamma_i$  (and  $\Sigma_{\mathbf{l}}$ ) are infinitesimal.

For the loss contribution to  $J_{\mathbf{k}}(\omega)$  we first consider only *the intrinsic part* (c.f. Eqs 1 and 43),

$$J_{\mathbf{k}}^1(\omega) = \sum_{q\mathbf{l}} \left| \sum_{\mathbf{l}'} \frac{-\langle \tilde{\mathbf{k}} | \Delta | \mathbf{l}' \rangle V_{\mathbf{l}'\mathbf{l}}^q}{\omega_q - \varepsilon_{\mathbf{l}} + \varepsilon_{\mathbf{l}'}} \right|^2 \delta(\omega - \omega_q - \varepsilon_{\mathbf{k}} + \varepsilon_{\mathbf{l}}). \quad (17)$$

The quadratic expression in the fluctuation potentials can be written in terms of the imaginary part of the self-energy

$$\text{Im} \Sigma_{\mathbf{l}\mathbf{l}'}(\omega) = \pi \sum_{q\mathbf{l}} V_{\mathbf{l}\mathbf{l}'}^q V_{\mathbf{l}'\mathbf{l}}^q \delta(\omega + \omega_q - \varepsilon_{\mathbf{l}}),$$

provided  $\omega < \mu$ , (see Eq. 19 in Ref. [22]). We can express  $\text{Im} \Sigma(\omega)$  in terms of  $\text{Im} W(\omega)$  as is clear from Eq. 39. This gives

$$J_{\mathbf{k}}^1(\omega) = \frac{1}{\pi} \sum_{\mathbf{l}\mathbf{l}'} \frac{\langle \tilde{\mathbf{k}} | \Delta | \mathbf{l}' \rangle \langle \tilde{\mathbf{k}} | \Delta | \mathbf{l} \rangle \text{Im} \Sigma_{\mathbf{l}\mathbf{l}'}(\varepsilon_{\mathbf{k}} - \omega)}{(\omega - \varepsilon_{\mathbf{k}} + \varepsilon_{\mathbf{l}})(\omega - \varepsilon_{\mathbf{k}} + \varepsilon_{\mathbf{l}'})}.$$

The condition  $\omega < \mu$  for  $\text{Im} \Sigma(\omega)$  translates to  $\varepsilon_{\mathbf{k}} - \omega < \mu$  in the above equation. This means that  $\omega > \varepsilon_{\mathbf{k}} - \mu$ , where  $\omega$  is the photon energy, which clearly is satisfied. Since  $\text{Im} \Sigma_{\mathbf{l}\mathbf{l}'}(\omega)$  is diagonal to a good approximation (Ref. [22]) we take

$$J_{\mathbf{k}}^1(\omega) = \frac{1}{\pi} \sum_{\mathbf{l}'} \frac{\left| \langle \tilde{\mathbf{k}} | \Delta | \mathbf{l}' \rangle \right|^2 \text{Im} \Sigma_{\mathbf{l}'}(\varepsilon_{\mathbf{k}} - \omega)}{(\omega - \varepsilon_{\mathbf{k}} + \varepsilon_{\mathbf{l}'})^2}. \quad (18)$$

We now make the following Ansatz for  $J_{\mathbf{k}}(\omega)$

$$\begin{aligned} J_{\mathbf{k}}(\omega) &= \sum_{\mathbf{l}} \left| \langle \tilde{\mathbf{k}} | \Delta | \mathbf{l} \rangle \right|^2 \int_{-\infty}^{\infty} \frac{dt}{2\pi} e^{i(\omega - \varepsilon_{\mathbf{k}} + E_{\mathbf{l}})t} \\ &\times \exp \left( \frac{1}{\pi} \int \frac{\text{Im} \Sigma_{\mathbf{l}}(\varepsilon_{\mathbf{l}} - \omega') (e^{-i\omega't} - 1) d\omega'}{(\omega')^2} \right). \end{aligned} \quad (19)$$

The integrand in the exponent is the function  $S_{\mathbf{l}}(-t)$  discussed in Refs [46] and [37],

$$S_{\mathbf{l}}(t) = \frac{1}{\pi} \int \frac{\text{Im} \Sigma_{\mathbf{l}}(\varepsilon_{\mathbf{l}} - \omega) (e^{i\omega t} - 1) d\omega}{\omega^2},$$

which for large  $t$  is

$$S_{\mathbf{l}}(t) = -\Gamma_{\mathbf{l}} |t| + i\alpha_{\mathbf{l}} \text{sgn}(t) - n_{\mathbf{l}}.$$

The quasiparticle behavior is set by the large  $t$  limit. Neglecting the asymmetry index  $\alpha_{\mathbf{l}}$  we have

$$J_{\mathbf{k}}^{QP}(\omega) = \frac{1}{\pi} \sum_{\mathbf{l}} \left| \langle \tilde{\mathbf{k}} | \Delta | \mathbf{l} \rangle \right|^2 e^{-n_{\mathbf{l}}} \frac{\Gamma_{\mathbf{l}}}{(\omega - \varepsilon_{\mathbf{k}} + E_{\mathbf{l}})^2 + \Gamma_{\mathbf{l}}^2},$$

which agrees with Eqs 6 and 7 since the factor  $\exp(-n_{\mathbf{l}})$  equals  $Z_{\mathbf{l}}$  to leading order. [37] The Ansatz to leading order also reproduces the intrinsic loss  $J_{\mathbf{k}}^1(\omega)$  in Eq. 18 apart from a normalization factor. The Ansatz further agrees with the result for intrinsic losses obtained earlier. [37] To have the intrinsic core electron spectrum we just replace the index  $\mathbf{l}$  by  $c$  in Eq. 19, and we have no summation.

For core electrons we can obtain *both the intrinsic and extrinsic contributions* [44], a detailed derivation is given in Appendix A in Ref. [4]. We found that Eq. 43 can be written

$$\begin{aligned} \tau_{qc}(\mathbf{k}) &= -\frac{V^q(\mathbf{r}_c)}{\omega_q} \langle \tilde{k}_z, \mathbf{K} | \Delta | c \rangle \\ &+ \frac{1}{i\kappa} \int_{-\infty}^{z_0} dz \psi_{k_z}^{\geq}(z) V(q_z, \mathbf{Q}, z) \psi_{\kappa}^{\leq}(z) \\ &\times \langle \kappa, \mathbf{K} - \mathbf{Q} | \Delta | c \rangle, \end{aligned}$$

provided we make a number of simplifying approximations. We have e. g. taken the crystal as translationally invariant parallel to the surface.  $\mathbf{K}$  and  $\mathbf{Q}$  are the

photoelectron and fluctuation potential momenta parallel to the surface, and  $\mathbf{r}_c$  is the position of the atom from which the core electron is excited. Further  $V(q_z, \mathbf{Q}, z)$  is the fluctuation potential  $V^q$ , and  $\psi_{\tilde{k}_z}^>(z)$  and  $\psi_{\tilde{k}_z}^<(z)$  are damped Blochfunctions,  $\psi_{\tilde{k}_z}^>$  decreasing towards the surface, and  $\psi_{\tilde{k}_z}^<$  decreasing towards the inner of the crystal. The momenta  $\tilde{k}_z$  and  $\kappa$  are equal when the quasi-boson energy and momenta are zero. We also take the dipole matrix elements as equal, and have

$$\begin{aligned} & \tau_{qc}(\mathbf{k}) \\ &= \left\langle \tilde{k}_z, \mathbf{K} | \Delta | c \right\rangle \\ & \times \left[ -\frac{V^q(\mathbf{r}_c)}{\omega_q} + \frac{1}{i\kappa} \int_{-\infty}^{z_0} dz \psi_{\tilde{k}_z}^>(z) V(q_z, \mathbf{Q}, z) \psi_{\tilde{k}_z}^<(z) \right], \end{aligned} \quad (20)$$

We can now obtain the result with both intrinsic and extrinsic contributions in the core electron case from the analysis of the intrinsic case by following the derivation from Eq. 17 to Eq. 19 and replacing  $-V^q(\mathbf{r}_c)/\omega_q$  by the full square parenthesis in Eq. 20. The result is given in Eq. 25. The expression in Eq. 43 for the extrinsic part for valence electrons is more involved to simplify. From the similar structure of the expressions for the core and valence electron cases we can however expect a similar qualitative behavior.

#### IV. THE USE OF THE ELECTRON ENERGY LOSS FUNCTION TO ESTIMATE LOSSES IN PHOTOEMISSION

It is a heavy computational task to do a priori calculations of the fluctuation potentials that are needed to evaluate extrinsic and intrinsic losses. Even when we limit ourselves (as we have done here) to expressions quadratic in the potentials, which can be described by  $\text{Im} W(\mathbf{r}, \mathbf{r}'; \omega)$ , the task is heavy since it is important to allow for the behavior of  $W$  at the surface. To avoid these difficulties, awaiting advances in computational techniques, we will develop approximations for  $W$  based on knowledge of the experimental energy loss function  $-\text{Im} \varepsilon^{-1}(\mathbf{q}, \omega)$ . [4] This is done in three steps. First we connect the bulk expression for  $\text{Im} W(\mathbf{r}, \mathbf{r}'; \omega)$  to  $\text{Im} \varepsilon^{-1}(\mathbf{q}, \omega)$ , and then we modify  $\text{Im} W(\mathbf{r}, \mathbf{r}'; \omega)$  to account for the surface. Unfortunately not much is known about energy loss at finite momenta, and one hence usually also have to make the third step of extrapolating the experimental  $\text{Im} \varepsilon^{-1}(\mathbf{q} = \mathbf{0}, \omega)$  values to finite  $\mathbf{q}$  values.

For a simple metal or a valence semiconductor, an "sp-system" [22], we take  $\varepsilon^{-1}$  as diagonal in  $\mathbf{q}$  space. We then have

$$\text{Im} W^{bulk}(\mathbf{r}, \mathbf{r}'; \omega) = \int e^{i\mathbf{q}(\mathbf{r}-\mathbf{r}')} v(\mathbf{q}) \text{Im} \varepsilon^{-1}(\mathbf{q}, \omega) d\mathbf{q}.$$

The fluctuation potentials for a bounded jellium have been discussed in Ref. [21]. The results for photoemission turned out to be fairly insensitive to the precise form

of the potentials as long as they went to zero at the surface. A reasonable choice is the Inglesfield one [44]

$$V^q(z) = F(z; q_z, Q) V_0^q,$$

$$F(z; q_z, Q) = [\cos(q_z z + \phi_q) - \cos \phi_q e^{-Qz}] \theta(z), \quad (21)$$

which is zero at the surface ( $z = 0$ ) and rapidly turns into a sine wave. The phase  $\phi_q$  is a certain function of  $q_z$  and  $Q$ . This leads us to replace the bulk expression

$$\text{Im} W(z, z'; \mathbf{Q}, \omega) \simeq \sum_{q_z} e^{iq_z(z-z')} \text{Im} W(q_z; \mathbf{Q}, \omega)$$

by

$$\begin{aligned} & \text{Im} W(z, z'; \mathbf{Q}, \omega) \\ & \simeq \sum_{q_z} F(z; q_z, Q) F(z'; q_z, Q) \text{Im} W(q_z; \mathbf{Q}, \omega). \end{aligned}$$

For correlated quasi 2D systems we are far from translational invariance in the  $z$  direction. Suppose we still have translational invariance parallel to the planes. We write the response between the induced charge density and the total (external plus induced) potential as  $\chi^0$ ,  $\rho^{ind} = \chi^0 V^{tot}$ , and approximate

$$\begin{aligned} \chi^0(z, z'; \mathbf{Q}) &= \chi_b^0(z - z'; \mathbf{Q}) \\ &+ \sum_{mn} w(z - cm - d_n) w(z' - cm - d_n) \tilde{\chi}_2^0(\mathbf{Q}). \end{aligned} \quad (22)$$

Here  $w(z) = |\phi_0(z)|^2$ , where  $\phi_0(z)$  is the ground state wave function for electrons localized in a 2D plane. The length of the unit cell in the  $z$  direction is  $c$ , and  $d_n$  gives the position of the layers inside a unit cell (when there are more than one layer). We thus write the response to the total potential as one part coming from extended 3D excitations plus one part from electrons which are localized in the  $z$  direction and only move in the planes. The variable  $\mathbf{Q}$  comes from the Fourier transform of  $\mathbf{R} - \mathbf{R}'$ , the coordinate distance in the plane. The susceptibility relating the induced charge density to the external potential  $\chi$ ,  $\rho^{ind} = \chi V^{ext}$  is related to  $\chi^0$  by  $\chi = \chi^0 + \chi^0 v \chi$ , and the inverse dielectric function is  $\varepsilon^{-1} = 1 + v \chi$ . Eq. 22 leads to a 3D bulk contribution to  $\text{Im} W(z, z')$ , plus a contribution  $v \chi_2 v$ , where the susceptibility  $\chi_2$  is calculated as if we only had the 2D planes and then replacing the bare Coulomb potentials in  $\chi_2$  with dynamically screened potentials from the embedding 3D electrons. We note that the bulk screened potential can be anisotropic since  $\chi_b^0(q_z, \mathbf{Q})$  can depend on both  $q_z$  and  $\mathbf{Q}$ , and not only on  $q_z^2 + \mathbf{Q}^2$ . If there is only one layer in the unit cell there is an explicit solution of the integral equation  $\chi_2 = \chi_2^0 + \chi_2^0 v \chi_2$ ,

$$\chi_2(q_z, q'_z) = \frac{1}{c} w(q_z) w(q'_z) \tilde{\chi}_2(q_z).$$



The variables  $\mathbf{Q}$  and  $\omega$  are suppressed,  $w(q_z)$  is the Fourier transform of  $w(z)$  and  $\tilde{\chi}_2(q_z)$  is a periodic function of  $q_z$ . Clearly  $w(0) = 1$ , and often it is reasonable to take  $w(q_z) = 1$  for all  $q_z$ . Due to the periodicity  $q_z$  and  $q'_z$  must differ by a reciprocal lattice vector. This means that if we know the diagonal part of  $\chi_2(q_z, q'_z)$  (from the loss function) we also know the full  $\chi_2(q_z, q'_z)$ . With several layers in the cell we have

$$\chi_2(q_z, q'_z) = \frac{1}{c} w(q_z) w(q'_z) \sum_{nn'} \tilde{\chi}_{nn'}(q_z) e^{iq_z d_n - iq'_z d_{n'}}.$$

Here  $\tilde{\chi}_{nn'}(q_z)$  is periodic, but the exponential factor is not. The diagonal part of  $\chi_2(q_z, q'_z)$  contains a sum of the matrix elements  $\tilde{\chi}_{nn'}(q_z)$  and thus the loss function cannot give us all of them. The diagonal elements of  $\tilde{\chi}_{nn'}(q_z)$  are equal, and if we neglect the non-diagonal elements (the coupling between the layers in a cell), again we have only one unknown quantity, which we can get from the loss function. Estimates for Bi2212 show that the nondiagonal elements are smaller than the diagonal ones [4], but still it is a fairly crude approximation to neglect them. In lack of other information than the loss function, we however feel forced to do so.

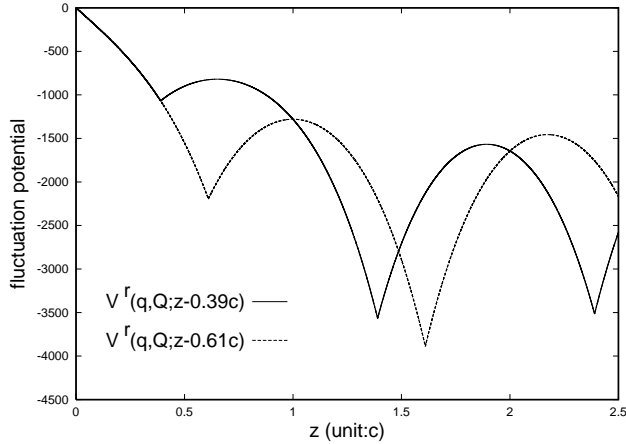


FIG. 3. The fluctuation potentials  $V^r(z - z_1)$  and  $V^r(z - z_2)$  where  $z_1$  and  $z_2$  are the positions of the first and second CuO layers in Bi2212. Note that in both cases the potentials are zero at the surface,  $z = 0$ .

To obtain the 2D contribution to  $W(z, z')$  we have to sum

$$\sum_{q_z q'_z} e^{-iq_z z} e^{iq'_z z'} v(q_z) \chi_2(q_z, q'_z) v(q'_z),$$

where the variables  $\mathbf{Q}$  and  $\omega$  still are suppressed. We split the summation over  $q_z$  into a sum (integral) over the Brillouin zone and a sum over reciprocal vectors  $G$ ,

$$W(z, z') - W^{3D}(z - z') \simeq \sum_n \int_{-\pi/c}^{\pi/c} V(z - d_n, q_z) V(z' - d_n, q_z) \tilde{\chi}_{1,1}(q_z) dq_z,$$

where

$$V(z, q_z) = e^{-iq_z z} V^p(z, q_z),$$

$$V^p(z, q_z) = \sum_G e^{-iGz} v(q_z + G) w(q_z + G). \quad (23)$$

The spacial dependence of the fluctuation potential is thus that of a Bloch wave, a plane wave times a periodic function  $V^p$ .  $V^p$  is a well-known function that can be obtained explicitly if we take  $w(q_z) = 1$ . We define real functions

$$V^r(z, q_z) = \text{Re} \left[ e^{-iq_z z + i\phi(q_z, z_0)} V^p(z, q_z) \right],$$

and choose the phaseshift  $\phi(q_z, z_0)$  to have  $V^r(z, q_z) = 0$  at the surface  $z = z_0$ . This procedure is like we would have taken  $F(z; q_z) = \sin[q_z(z - z_0)]$  which is not unreasonable. In summary this gives us

$$\text{Im } W^{2D}(z, z') \simeq \sum_n \int_{-\pi/c}^{\pi/c} V^r(z - d_n, q_z) V^r(z' - d_n, q_z) \text{Im } \tilde{\chi}_{1,1}(q_z) dq_z,$$

where  $\text{Im } \tilde{\chi}_{1,1}(q_z)$  can be obtained from the loss function. We should have replaced  $v(q_z)$  by a screened potential  $W(q_z)$  everywhere, but since we have the same replacements in the expression for loss function, this is of no consequence. The coupling functions  $V^r(z)$  are quite different from the functions  $V^q(z)$  in Eq. 21 for the 3D case. As shown in Fig. 3 they look more like a superposition of surface plasmon functions centered at the different 2D layers than a sine wave.

The third step of extrapolating to finite momenta also involves considerable uncertainty. It is however important to do some estimates of the effects of dispersion since we know that for an electron gas it makes a difference of a factor of two for the mean free path. For an electron gas the plasmon pole model is fairly good, also when a simple quadratic dispersion is used

$$\text{Im} \frac{-1}{\varepsilon(q, \omega)} \simeq \delta(\omega - \omega_q), \quad \omega_q = \omega_p + q^2/2.$$

Often a one mode description is not good enough. One can then use a sum of Drude functions, which further include damping of the quasi-boson modes,

$$\text{Im} \frac{-1}{\varepsilon(q, \omega)} = \sum_n c_n^0 \frac{\omega \Gamma_n(q)}{(\omega^2 - \omega_n^2(q))^2 + \omega^2 \Gamma_n^2(q)},$$

$$\omega_n(q) = \omega_n^0 + q^2/2, \quad (24)$$

as suggested by Ritchie and Howie [49] and others. [50] The dispersion of  $\omega_n(q)$  is somewhat ad hoc, however for large  $q$  it has the correct form, following the Bethe ridge. Also for  $\Gamma_n(q)$  some dispersion could be used. The coefficients  $c_n^0$ ,  $\omega_n^0$ , and  $\Gamma_n(0)$  can be determined by fitting to the energy loss function  $-\text{Im } \varepsilon^{-1}(q = 0, \omega)$ .

## V. INTERFERENCE BETWEEN INTRINSIC AND EXTRINSIC LOSSES

### A. Localized strongly correlated systems

There is a fundamental difference between photoemission from solids and from localized systems like atoms or molecules. The interaction between the photoelectron and the target always goes to zero at high kinetic energies. In solids this decreasing interaction is compensated by the longer distance the electron travels, due to its longer mean free path, before it leaves the solid (assuming that the light penetrates much deeper into the solid than the mean free path). Thus while at high energy the photoelectron coupling can be neglected for a localized system, it never becomes negligible for a solid.

An extensive literature has appeared on near-threshold behavior of satellites in atomic spectra, with a landmark paper from 1965 by Carlson and Krause [51] where they observed the characteristic shake-up behavior for the first time. They showed that the intensity of the shake-up satellite in K-shell excitation of the Ne atom rouse slowly from zero at threshold to its sudden approximation limit at some 200 eV higher energy. The data were plotted in units of the "excitation" energy  $E_0$  of the satellite final state relative to the main line ( $E_0 = 50$  eV in the Ne case). The onset of satellite intensity was studied particularly in the 80's when good synchrotron sources had become available. Stöhr, Jaeger and Rehr in 1983 [52] made a systematic study of the energy dependence of a core level shake-up feature (the K spectrum of  $N_2$  on  $Ni(100)$ ) with a much smaller value of  $E_0$  (5 eV). Also here the approach to the sudden limit was found to occur within a few unit of  $E_0$ . Reviews of the atomic work on threshold satellites have been given by Becker and Shirley. [53], [54] The picture that evolved was complex with rapid variations in satellite intensities near threshold. Much of the complexity is however related to Rydberg levels and post collision effects, which have less relevance in solids.

The satellite turn-on was recently studied in detail for a numerically exactly soluble model that should be generic for a class of strongly correlated solid state systems. [3] The model has a charge transfer excitation, and is relevant for transition metal halides, rare earth compounds, chemisorption systems, and high  $T_c$  compounds. It is modelled by three electron levels, one core level and two outer levels. When the core hole (3s) is created, the more localized outer level (d) is pulled below the less localized level (L). The spectrum has a leading peak corresponding to a charge transfer between L and d ("*shake-down*"), and a satellite corresponding to no charge transfer. The "*conjugate shake-up*" mechanism (optical transition between two localized levels (s and d) plus shake-up from a localized level (L) to the continuum) analyzed by Thomas [55] is not relevant in our case since an s-d transition is optically forbidden. The crucial feature of the model is the

dynamic Coulomb interaction between the photoelectron and the d and L levels, i. e. the interaction that causes extrinsic losses. The calculations were done with parameters relevant to different copper-dihalide compounds ( $CuBr_2$ ,  $CuCl_2$ ,  $CuF_2$ ), and showed a rapid approach (see Fig. 4) to the sudden limit within 5-10 eV, which is in accord with the Stöhr et al results. To the extent that the localized system described by this model can be regarded as decoupled from the rest of the (3D) solid, this means that above say 10 eV extrinsic losses and interference effects are associated only with 3D extended excitations.

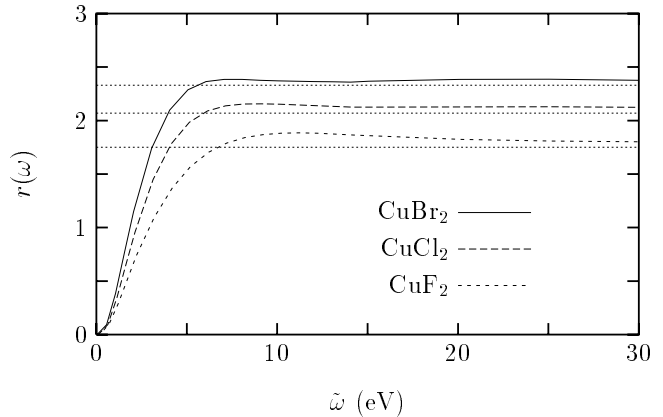


FIG. 4. The ratio  $r(\omega)$  between the satellite and the main peak photocurrents for some divalent copper compounds. The energy is measured from the threshold for satellite onset, and the horizontal lines give the sudden limit.

With an exactly solvable model some detailed mechanisms for the satellite turn-on could be studied. Since the transition takes place at such low energies it turned out that the variation of the dipole matrix element gave effects comparable to that of the dynamic photoelectron coupling. When the dipole matrix effect dominates (intrinsic case), the onset is determined by  $E_0$  as long as  $E_0$  is smaller or comparable to the characteristic energy  $E_d = 1/R_d^2$  where  $R_d$  gives the length scale of the dipole matrix element. For  $E_0$  larger than  $E_d$  it is instead  $E_d$  which gives the characteristic onset energy. The strength of the satellite relative to that of the main line obtained with the full model divided by the result when only the matrix element was considered, showed curves starting at 1 at zero energy which could have sizable humps (extrinsic effects) at an energy of order  $E_d$ . Attempts to describe these effects by a semiclassical approximation were not successful, and no simple picture in time space evolved. Lowest order perturbation theory on the other hand succeeded in giving some qualitative understanding. One conclusion is that  $E_0$  may not always be the correct scaling parameter for satellite onset.

## B. Weakly correlated solids

The transition from the adiabatic to the sudden limit in core electron photoemission for weakly correlated systems was recently studied. [21] The theory is fully quantum mechanical and includes the interference between intrinsic and extrinsic losses (QM). It is a general theory for weakly correlated systems and describes not only plasmon losses but losses to density fluctuations in general like those from electron-hole excitations. The actual calculations were done for an atom embedded in a semi-infinite jellium. For such a simple model explicit and detailed results could be obtained. The limit expression when the interference term in Eq. 20 was neglected (BS), gives essentially the same approximation as discussed by Berglund and Spicer [31] and used by Penn. [39] Comparison was also made with results from the semi-classical theory (SC). In this theory the photoelectron is taken to travel with a steady speed on a straight trajectory, and the photoelectron losses are identified with the excitations caused in the solid by the external perturbation from the moving classical photoelectron. In Sect. III we presented general results, partly based on Ref. [21].

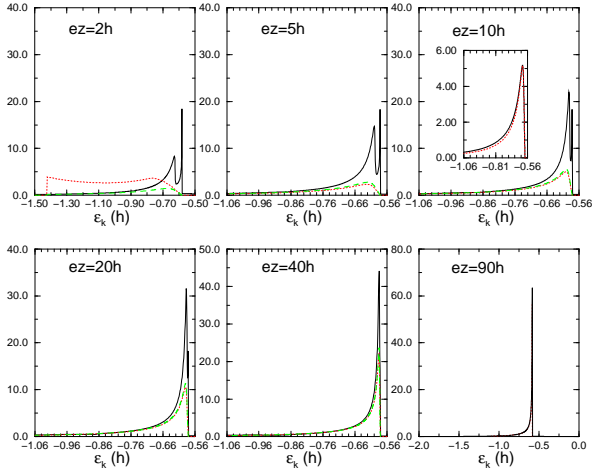


FIG. 5. Satellite part of the photoelectron spectrum for Al ( $r_s = 2.07$ ) from lowest order perturbation theory showing the contribution from bulk plasmons as function of photoelectron energy (the zero of the energy scale is at the quasi-particle energy), for different photon energies. We show results for three different approximations, fully quantum mechanical (QM) from Eq. 26 (dotted curves); neglecting interference (BS) from Eq. 27 (solid curves); and semiclassical (SC) from Eq. 28 (dashed curves). The inset in the  $ez = 10$  curve shows results with two different polarization potentials (see Ref.[21]).

The photocurrent for the core electron case is

$$J_{\mathbf{k}}(\omega) = \left| \langle \tilde{\mathbf{k}} | \Delta | c \rangle \right|^2 \int_{-\infty}^{\infty} \frac{dt}{2\pi} e^{i(\omega - \varepsilon_{\mathbf{k}} + E_c)t} \quad (25)$$

$$\times \exp \left( \frac{1}{\pi} \int g_{QM}(\omega') (e^{-i\omega't} - 1) d\omega' \right).$$

We have used Eq. 20, and replaced the Bloch functions with plane waves, to find

$$g_{QM}(\omega) = \quad (26)$$

$$\sum_q \left| \frac{-V^q(z_c)}{\omega_q} + \frac{1}{i\kappa} \int_{-\infty}^{z_c} dz e^{i(\tilde{\mathbf{k}} - \boldsymbol{\kappa})(z - z_c)} V^q(z) \right|^2 \delta(\omega - \omega_q).$$

Here  $z_c$  is the position of the atom from which the photoelectron comes,  $q$  labels the fluctuation potentials  $V^q$  (mostly taken from Eq. 21),  $q = (q_z, \mathbf{Q})$ , and

$$\tilde{\kappa}^2 = k_z^2 + 2(|V_0| + i\Gamma_f),$$

$$\kappa^2 = k_z^2 + 2(|V_0| + \omega_q + i\Gamma_2) - |\mathbf{Q}|^2.$$

Further  $V_0 = \langle V_{eff} \rangle_{average}$ ,  $V_{eff}$  is the effective crystal potential,  $\Gamma_f = |\text{Im} \Sigma(\varepsilon_{\mathbf{k}} + |V_0|)|$ , and  $\Gamma_2 = |\text{Im} \Sigma(\varepsilon_{\mathbf{k}} + |V_0| + \omega_q)|$  (c. f. Eq. 8). The photoelectron is taken to leave the solid at right angle to the surface.

### Satellite spectrum (exponential expression)

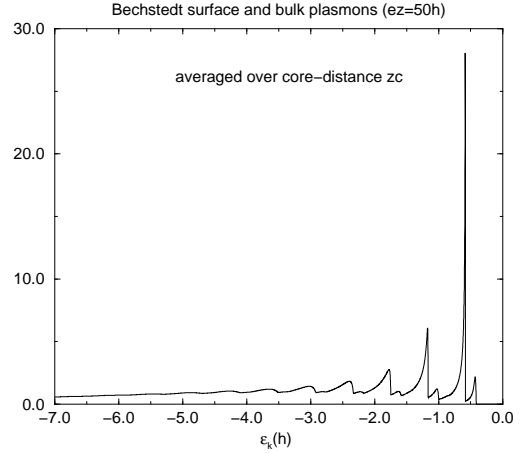


FIG. 6. Satellite spectra from the exponential expression in Eq. 25 in a plasmon pole approximation neglecting electron-hole contributions but including both surface and bulk plasmons. The spectra are averaged over core hole position and for a high photon energy ( $ez = 50$ ).

In the high energy limit the interference terms in Eq. 26 drop out and we have [21], [56]

$$g_{BS}(\omega) = \frac{\alpha(\omega)}{\omega} + z_c \tau(\varepsilon, \omega), \quad (27)$$

where  $\alpha(\omega)$  is the function giving the intrinsic spectrum ( $\alpha(0)$  is the MND singularity index [23]), and  $\tau(\varepsilon, \omega)$  is the differential inverse mean free path (see e. g. Ref. [57]),

$$\tau(\varepsilon, \omega) = \frac{1}{\pi\varepsilon} \int \frac{dq}{q} \text{Im} \left[ \frac{-1}{\varepsilon(q, \omega)} \right].$$

Eq. 27 gives a result roughly the same as that obtained from the transport theory used by Penn. [39] Finally the semi-classical theory with the photoelectron as a perturbing charge on a straight trajectory gives [21]

$$g_{SC}(\omega) = \int_q \left| \frac{-V^q(z_c)}{\omega_q} + \frac{1}{iv} \int_{-\infty}^{z_c} dz e^{-i\omega_q(z-z_c)/v} V^q(z) \right|^2 \delta(\omega - \omega_q), \quad (28)$$

where  $v$  is the photoelectron velocity.

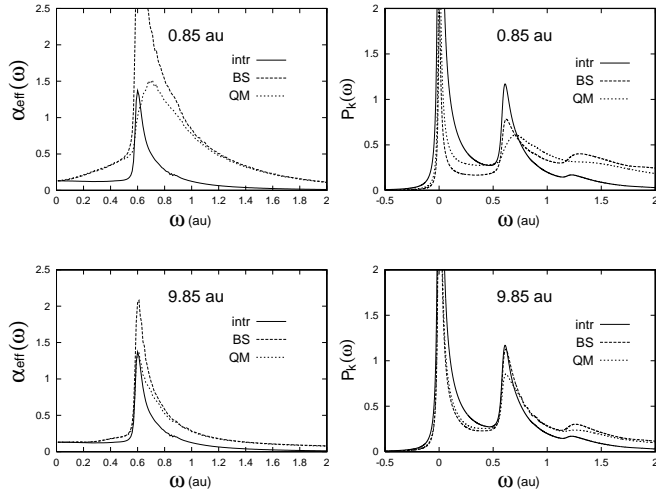


FIG. 7. Curves of  $\alpha_{eff}(\omega)$  and  $P_k(\omega)$  for Al metal with a photoelectron energy of 0.85 au (upper panel) and 9.85 au (lower panel). The  $P_k(\omega)$  curves are for given  $k$  values as functions of  $\omega$ , i. e. they are "constant final state spectra" (CFS).

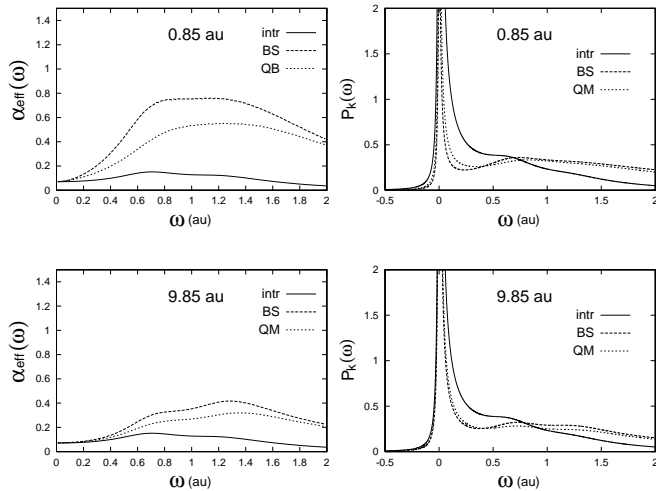


FIG. 8. The same results as in Fig. 7 for Cu metal.

In Fig. 5 we show results for the bulk plasmon satellite in the three approximations. The results are from the lowest order term in expanding the exponential in Eq. 25 using a plasmon pole approximation (no electron-

hole pairs and no surface plasmons). Actually the results from the exponential expression and lowest order theory are identical apart from a constant factor in the energy range up to the second satellite peak. The semi classical theory works almost perfectly except at lower photon energies (see curve with  $ez = 2$ ), while the Berglund and Spicer transport theory works poorly until the energy is very high (of order keV). The quantity  $ez$  is the maximum energy that the photoelectron can have with a given photon energy.

In Fig. 6 we show the satellite region over an extended energy range at a high photon energy ( $ez = 50$ ), calculated with the exponential expression in Eq. 25, and averaged over core hole position. We see the strong bulk plasmons preceded by the weaker surface plasmons. The higher order plasmon peaks become broader and broader. The very sharp first and second order peaks will become broader when plasmon damping and electron-hole excitations are accounted for.

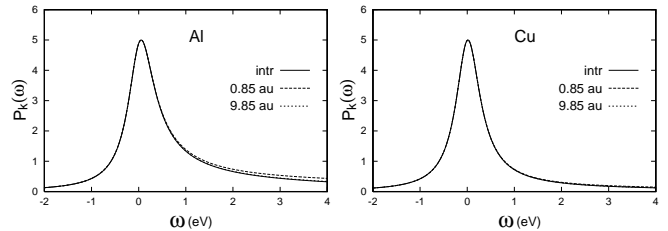


FIG. 9. Curves of the asymmetric quasi-particle peak for Al metal (left) and Cu metal (right). The curves have a 300 meV Lorentzian broadening, and give results for emission from an atom 10 au from the surface. Results for a photoelectron kinetic energy of 0.85 and 9.85 au, and also when only the intrinsic contribution (independent of photoelectron energy) is included.

Al metal is rather special in having a very sharp plasmon peak carrying most of the loss spectral strength (see e. g. Fig 4.14 in Ref. [35]). To study the effect of the shape of the loss function we did some comparisons between Al and Cu. We define an "effective" singularity function by  $\alpha_{eff}(\omega) = \omega g_{QM}(\omega)$  which includes both intrinsic and extrinsic amplitudes, and thus depends on the photoelectron energy. In Fig.7 we show  $\alpha_{eff}(\omega)$  for Al at two different photoelectron energies, and compare results from taking only the intrinsic contribution (intr) with the BS and QM cases. Clearly both extrinsic and interference effects are strong also at the higher energy. In Fig. 7 we also show the photocurrent as function of the photon energy obtained with the exponential expression, Eq. 19 at the two photoelectron energies (CFS mode). The same results for Cu are shown in Fig. 8. It is clear that extrinsic and interference effects are just as strong in Cu as in Al. The difference in the loss spectra of the two metals however shows in the shape of the satellites, the Cu satellite is featureless as could be expected. In Fig. 9 we show both the intrinsic (intr) and the quantum me-

chanical (QM) results for the quasi-particle peaks for Al and Cu, broadened by a Lorentzian of FWHM=600 meV, and for two photoelectron energies. It is clear that both FWHM and asymmetry in practice are unaffected both by photoelectron energy and by extrinsic losses.

### C. Strongly correlated quasi two-dimensional solids

In many high temperature superconductors (HTC) we have layered materials with planes of CuO which are active in superconductivity. Much theoretical work concentrates on the electronic correlations in these quasi-2D CuO planes, and there are many interesting relations between properties found theoretically in purely 2D systems and experiment. To interpret photoemission data the full 3D crystal should however be taken into account. In a recent study of Bi2212 we find strong effects on the threshold line shape due to low energy excitations connected with the coupling between the planes, effects which do not appear in a pure 2D treatment. [4] The effects can be seen as external if we consider photoemission from one layer and regard the layers outside as an external system, or dominantly intrinsic if we look at the system as three-dimensional. The effect we discuss is different from that considered by Haslinger and Joynt [58], who consider ohmic losses of the photoelectron occurring after the electron has left the solid.

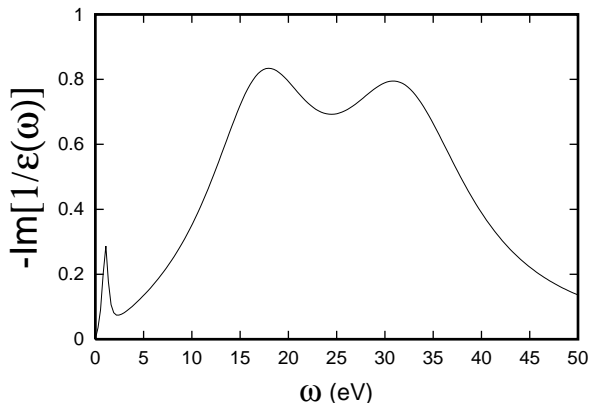


FIG. 10. The loss function for Bi2212 as parametrized by Norman et al.[59]

The low energy part of the photoemission spectrum comes from exciting electrons in a 2D layer of Bi2212. The one electron states are then quite localized in the  $z$  direction, and the shake-up and loss effects are assumed to be similar to those in a core electron spectrum. As further motivation for this assumption we can compare with results for simple metals. In Sect. III we noted that the valence electron satellite structure in simple metals is very similar to the core electron one. Further the valence electron quasi-particle line shape, away from the Fermi level, is markedly asymmetric just like a core line. [46] For electrons at the Fermi level, which is an important

case, we can however not rest on a comparison with valence electrons but have to rely on the localization in the  $z$  direction.

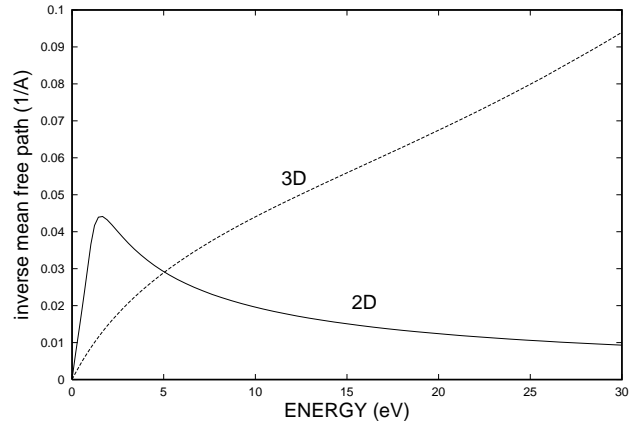


FIG. 11. The contributions to the inverse mean free path  $1/\lambda$  from the 2D (full drawn) and 3D (dashed) terms in the case of Bi2212.

The calculations for Bi2212 take as input data a three term parametrization (see Eq. 24) made by Norman et al [59] of the loss spectrum obtained by Nücker et al [60]. The parametrized curve is shown in Fig. 10. The first sharp peak describes 2D plasma vibrations, and the linear small  $\omega$  part the acoustic plasmons coming from coupling between the 2D layers. In Fig. 11 we show the contributions to inverse mean free path coming from the 2D part (the first term), and the 3D part (the second and third terms). It is clear that at about 20 eV, where photoemission measurements usually are done, the 3D contribution dominates. As discussed in the introduction, we take the statevectors as direct products, and write for the initial and final states,

$$|N_B\rangle |N_{2D}\rangle, |N_B^*, s_1\rangle |N_{2D} - 1, s_2\rangle |\mathbf{k}\rangle. \quad (29)$$

Here  $|N_{2D}\rangle$  is the state vector for the electrons in one particular layer at a distance  $z_0$  ( $z_0 > 0$ ) from the surface (the one from which the photoelectron comes), and  $|N_B\rangle$  the state vector for the remaining (bulk) electrons which move in 3D.  $|N_{2D} - 1, s_2\rangle$  is an excited state  $s_2$  of the particular layer, and  $|N_B^*, s_1\rangle$  an excited state  $s_1$  of the bulk electrons. The star indicates that these electrons move in the presence of a localized hole at  $\mathbf{r} = (\mathbf{0}, z_0)$ , and thus is an eigenfunction of a different Hamiltonian than that for  $|N_B\rangle$ . Finally  $|\mathbf{k}\rangle$  is the photoelectron state.

Assuming that the 2D part is like a core level, we could derive an expression for the photocurrent as a convolution between the 2D current  $J_{\mathbf{k}}^{2D}(z_0, \omega)$  and an *effective broadening function*  $P_{\mathbf{k}}(z_0, \omega)$ ,

$$J_{\mathbf{k}}(z_0, \omega_{phot}) = \int J_{\mathbf{k}}^{2D}(z_0, \omega') P_{\mathbf{k}}(z_0, \omega_{phot} - \omega') d\omega'. \quad (30)$$

A delta function peak  $\delta(\omega - \varepsilon_0 - \varepsilon_{\mathbf{k}})$  in  $J_{\mathbf{k}}^{2D}(z_0, \omega)$  will hence give a contribution  $P_{\mathbf{k}}(z_0, \omega_{phot} - \varepsilon_0 - \varepsilon_{\mathbf{k}})$  to the photocurrent. Summing up to an exponential expression we have

$$P_{\mathbf{k}}(\omega) = e^{-z_0/\lambda - a_{3D}^{intr}} \int \frac{dt}{2\pi} e^{-i\omega t} \quad (31)$$

$$\times \exp \left[ \int_0^\infty \alpha_{2D}(\mathbf{k}, z_0; \omega') \frac{e^{i\omega' t} - 1}{\omega'} d\omega' \right. \\ \left. + \int_{\omega_{th}}^\infty \alpha_{3D}(\mathbf{k}, z_0; \omega') \frac{e^{i\omega' t}}{\omega'} d\omega' \right].$$

The 3D contribution is somewhat arbitrarily cut at a threshold value of  $\omega_{th} = 0.1$ . We have replaced  $e^{i\omega' t} - 1$  by  $e^{i\omega' t}$  in the 3D term. The reason is that in the high energy limit we have

$$\int_{\omega_{th}}^\infty \frac{\alpha_{3D}(\mathbf{k}, z_0; \omega)}{\omega} d\omega = a_{3D}^{intr} + z_0/\lambda, \quad (32)$$

provided we neglect the contribution to the mean free path  $\lambda$  coming from 2D excitations. This, as we just remarked, is reasonable at photoelectron energies of 20 eV and higher. Since the 2D and 3D contributions add in an exponent we can write  $P_{\mathbf{k}}(z_0, \omega)$  as a convolution,

$$P_{\mathbf{k}}(z_0, \omega) = e^{-z_0/\lambda - a_{3D}^{intr}} \\ \times \int P_{\mathbf{k}}^{2D}(z_0, \omega - \omega') P_{\mathbf{k}}^{3D}(z_0, \omega') d\omega'.$$

For  $P_{\mathbf{k}}^{3D}$  we make a Taylor expansion, and keep only the low order result,  $P_{\mathbf{k}}^{3D}(z_0, \omega) = \delta(\omega) + \alpha_{3D}(z_0, \omega)/\omega$ . We have then omitted the multiple quasi-boson excitations starting at  $\omega = 2\omega_{th}$ . Since  $P_{\mathbf{k}}^{2D}$  is normalized to unity, and consists of a peak that is sharp compared to  $\alpha_{3D}$ , we can write

$$P_{\mathbf{k}}(z_0, \omega) \simeq e^{-z_0/\lambda - a_{3D}^{intr}} \left[ P_{\mathbf{k}}^{2D}(z_0, \omega) + \frac{\alpha_{3D}(\mathbf{k}, z_0; \omega)}{\omega} \right]. \quad (33)$$

The extrinsic contribution to  $\alpha_{2D}(\mathbf{k}, z_0; \omega)$  can be neglected, and the intrinsic contribution has a  $z_0$  but no  $\mathbf{k}$  dependence. There is a competition between a declining function  $\exp(-z_0/\lambda)$  and an increasing function  $\alpha_{2D}(z_0, \omega)$  making the contribution from the second layer dominate. We approximate  $\alpha_{2D}(z_0, \omega)$  by a rectangular function,  $\alpha_0 \theta(\omega_0 - \omega)$  independent of  $z_0$ , and broaden with a Lorentzian of width  $\Gamma$  ( $FWHM = 2\Gamma$ ). As parameters we use  $\alpha_0 = 0.255$  and  $\omega_0 = 0.08$ . For  $\omega < \omega_0$  we then have the Doniach-Sunjc expression [61],

$$P_{\mathbf{k}}^{2D}(\omega) = C(\alpha_0) \frac{\cos[\pi\alpha_0/2 - (1 - \alpha_0) \arctan(\omega/\Gamma)]}{\left(1 + (\omega/\Gamma)^2\right)^{(1-\alpha_0)/2}}, \\ C(\alpha_0) = \frac{e^{-\gamma\alpha_0}}{(\alpha_0 - 1)! \omega_0^{\alpha_0} \Gamma^{1-\alpha_0} \sin[\pi\alpha_0]} \quad (34)$$

where  $\gamma = 0.577$  is the Euler constant. For  $\omega > \omega_0$   $P_{\mathbf{k}}^{2D}(\omega)$  only has a weak tail with less than 10% of the norm (for  $\alpha_0 < 0.4$ ). The coefficient  $C(\alpha_0)$  was derived in Ref. [56].

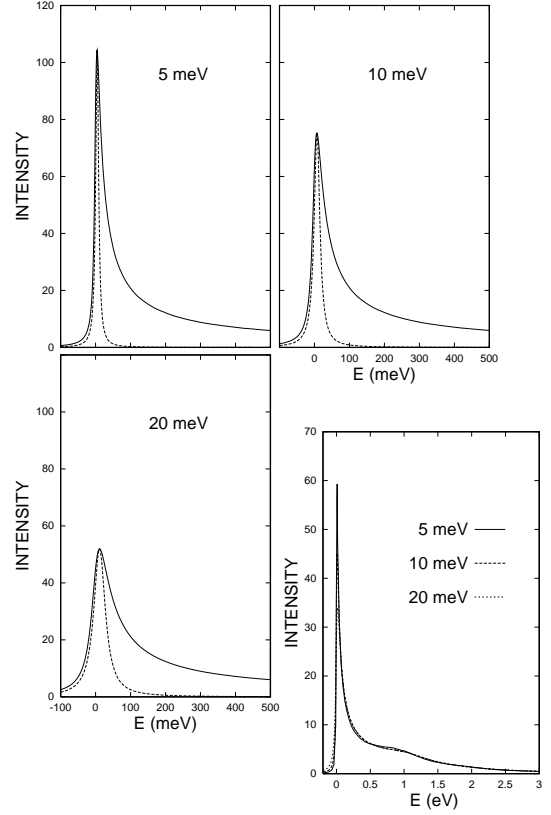


FIG. 12. The effective loss function  $P_{\mathbf{k}}^{2D}(\omega)$  convoluted with Lorentzians of different widths  $\Gamma$  (5, 10, and 20 meV). Also the Lorentzians are shown. The photoelectron energy is 0.85 au.

$P_{\mathbf{k}}^{2D}(\omega)$  is the function that broadens a  $\delta$ -function peak in  $J_{\mathbf{k}}^{2D}(\omega)$ . If  $J_{\mathbf{k}}^{2D}(\omega)$  has a Doniach-Sunjc singular shape the broadening with  $P_{\mathbf{k}}^{2D}(\omega)$  still gives Eq. 34 but with an  $\alpha_0$  that is the sum of the alphas in  $J_{\mathbf{k}}^{2D}$  and in  $P_{\mathbf{k}}^{2D}(\omega)$ . This is so because the time transform of a power law singularity  $\omega^{-(1-\alpha_0)}$  is  $t^{-\alpha_0}$ , and a convolution in frequency space is a product in time space.

In Fig. 12 we show the sum for the first four layers of the 2D contributions  $\exp(-z_0/\lambda - a_{3D}^{intr}) P_{\mathbf{k}}^{2D}(\omega)$  broadened with different Lorentzians. The 3D terms are not included except for the (all important) mean free path factor. In the first three panels with a limited energy region (up to 500 meV) we have used the rectangular approximation for the  $\alpha_{2D}$  contributions. In the last panel with a larger energy range the full evaluation was done since it is superior to the rectangular model for energies above 0.5 eV. Also the Lorentzians are shown to ease the estimate of the size of the asymmetries. It is clear that we have a sizeable line asymmetry, and also a long tail extending over several eV.

In the superconducting state the loss function should have a gap. We mimic this gap by using a rectangular alpha function

$$\alpha_{2D}(\omega) = \alpha_0 \theta(\omega - \omega_{sc}) \theta(\omega_0 - \omega), \quad (35)$$

still using  $\alpha_0 = 0.255$  and  $\omega_0 = 0.08 \text{ au} = 2.2 \text{ eV}$ . For the gap  $\omega_{sc}$  we take  $\omega_{sc} = 70 \text{ meV}$ . In Fig. 13 we show the corresponding  $P_k^{2D}(\omega)$  broaden with a Lorentzian of width  $\Gamma = 15 \text{ meV}$ . Our choice of parameters is only made to illustrate the qualitative behavior to be expected. The curve clearly shows the peak-dip-hump lineshape found experimentally (for a recent reference see e.g. [62])

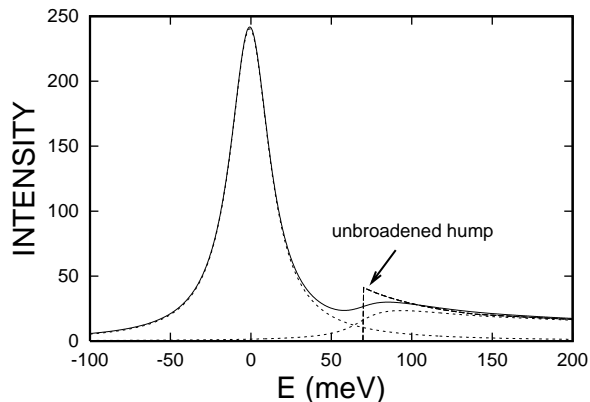


FIG. 13. The effective loss function  $P_k^{2D}(\omega)$  for a gapped spectrum using the parametrization in Eq. 35. The Lorentzian broadening is  $\Gamma = 15 \text{ meV}$ .

Recently it has been possible to obtain very accurate tunneling data from Bi2212, and it is of interest to compare these data with the PES satellites (Ref. [63]), since the tunneling data also show peak-dip-hump structures. [64] PES and tunneling are basically different spectroscopies. There can however be qualitative similarities since in both cases the electrons couple to 3D quasi-boson excitations like phonons, electron-hole pairs, plasmons, magnons etc. In our treatment of PES we take the properties of a particular 2D layer as given and study the effect to low order of the sudden appearance of a hole in the 2D system on the quasi-bosons (intrinsic excitations) as well as of the coupling of the photoelectron leaving this layer to the quasi-bosons (extrinsic excitations), and their interference. We found that the intrinsic contributions dominate for small excitation energies.

Tunneling is traditionally described by a spectral function which involves matrix elements of the electron annihilation operator between the initial state and the excited states. [65], [23] The excited states consist of a 2D layer state with a hole, and some state of the quasi-bosons in the presence of a localized hole. In lowest order perturbation theory the probability for a final state with excited quasi-bosons is given by the first term in Eq. 20. This means that *the intrinsic contribution to PES and the tunneling currents are the same* except for the mean

free path effect in PES shown in Eq. 33, and the summation over momenta in tunneling giving the density of states, DOS. In PES on the other hand, we have momentum conservation from the dipole matrix element. As mentioned above, we modify this analysis valid for the normal state, by simply assuming that the loss function should have a gap in the superconducting state.

In Bi2212 we have a van Hove singularity (VHS) at the Fermi level, which makes the difference between DOS and momentum conservation of less importance (there might actually even be two VHS if the two *CuO* planes at 3 Å apart produce a significant splitting). More important is that in PES the electrons come from a thin surface region (of the order of the mean free path) while in tunneling they may come from an extended region which can be hundreds of Å, and that the coupling functions  $V(z)$  have a slow approach to their bulk limit (Fig. 3). Additionally there are two energy gaps (superconducting gap and pseudogap), which further complicates the picture. It is clear that PES and tunneling structures cannot be quantitatively the same, but since the same quasi-bosons are involved, there may well be qualitative similarities even though the coupling strengths can be different. We remind that we have taken the spectral function for the 2D system (the function often calculated by theoreticians using say a t-J model) as a sharp peak, and any peak structure in  $J_{2D}(\omega)$  has to be convoluted with the effective broadening function  $P_{2D}$ . In our analysis we have only treated the plasmons for the simple reason that the experimental loss data at hand did not have resolution enough to show phonons and other low energy excitations.

## VI. CONCLUDING REMARKS

When we go beyond the common procedure of comparing the spectral function with photoemission, there are a number of definitions and distinctions that have to be introduced. In the *one-step approximation* only the quasi-particle peak and the dipole matrix element are included but no intrinsic or extrinsic losses. In the *intrinsic approximation* the full spectral function including its tail from intrinsic losses, as well as the dipole matrix element are included, but no extrinsic losses. In the *sudden approximation* (or *Berglund-Spicer* model) the spectral function is taken as a source term in a transport problem, or roughly equivalently we make a convolution between spectral function and the extrinsic loss function. The dipole matrix element is taken as independent of loss energy. The *adiabatic approximation* somehow describes the behavior at threshold, but there is no simple approximation scheme to do this. When the losses come from extended excitations the satellite in photoemission has contributions both from intrinsic and extrinsic *amplitudes*. A *semi-classical approximation* puts the photoelectron on a trajectory, and the losses are calculated

with the photoelectron as an external perturbation. It should be noted that there is considerable ambiguity in the literature concerning these definitions.

In this paper we discuss photoemission in general, we explore the limits of the sudden approximation, and we analyze the role of extrinsic losses. It is not a comprehensive treatment, that would require much more space, and we concentrate on some problems of broad interest. Thus in core electron photoemission we e.g. do not take account of the finite core electron lifetime. This lifetime can cause spectacular effects if phonon energies are of the same order as the lifetime width. [66] It can also cause large effects if there e.g. are Koster-Kronig decay channels, and two nearby discrete levels (say  $2p_{1/2}$  and  $2p_{3/2}$ ). [67] There are many resonance effects in d and f electron systems, some involving atoms on different sites like multiatom resonance PES. [68] We have omitted this large topic. For a general review see Ref. [69]

We study in some detail how the three-dimensionality of a quasi-2D solid, Bi2212, influences its photoemission. We have earlier found that for a strongly correlated *localized* system the sudden approximation is reached rather quickly, at about 10 eV [3]. For a weakly correlated system on the other hand, like an sp-metal or semiconductor, the sudden limit in core electron photoemission is approached very slowly, on the keV scale. [21] The slow approach is connected with strong destructive interference between the intrinsic and extrinsic channels for plasmon production. The cancellation is particularly strong for small momentum plasmons where the long-wave plasmons are excited by the average potential from the core hole and photoelectron, which is zero [70]. When we compare the satellites of Al and Cu we find that the latter have about the same strength but are structureless. The asymmetric lineshape in core electron photoemission from metals is, on the other hand, hardly affected by the external loss processes [21].

We are interested in energies where the sudden limit is reached for the strongly correlated layer from which the photoelectron comes, and derive an expression for the photocurrent as a convolution of the sudden approximation for the current from the layer with an effective loss function,  $P_{\mathbf{k}}(\omega)$  (Eq. 30). We assume, as far as the loss properties are concerned, that the photoelectron comes from a localized position. In our specific example, Bi2212, the  $c$  value is 15.4 Å (neglecting crystallographic shear), and almost all contributions come from the first unit cell. The two first *CuO* layers are at 0.39  $c$  and 0.61  $c$  from the surface (which is between two *BiO* layers). [71]

To obtain  $P_{\mathbf{k}}(\omega)$  we use a previously developed method based on a quasi-boson model, where the electron-boson coupling is given by fluctuation potentials related to the dielectric response function [22]. We find that the energy loss function, which we take from experimental data, can be related to the screened potential which we need to calculate the (intrinsic and extrinsic) losses in photoemission. The fluctuation potentials related to the electrons

in the layers are universal functions, which are easily calculated. They have some resemblance to a surface plasmon potential, but penetrate the whole solid and have the Bloch wave symmetry. We use the real part (or equivalently the imaginary part) of a phase shifted bulk potential to get a potential which is zero at the surface, and mimics the potential we have in a finite solid.

We have extrapolated results from electron energy loss experiments for  $q=0$  to finite values of  $q$ . This inclusion of dispersion makes the mean free path considerably longer than obtained by Norman et al [59], about 12 Å rather than 3 Å, at say 20 eV (Fig. 2). Measurements by the ITR-2PP technique [72] give a lifetime of  $\tau = 10$  fs at an energy  $\varepsilon = 3$  eV above the Fermi surface. The mean free path is  $\lambda = v\tau$ . Converting energy to velocity by  $mv^2/2 = \varepsilon$  gives a mean free path  $\tau = 103$  Å as compared to our result of about 17 Å at that energy. This is an indication that our values rather are on the low side. It is however hard to know what is the correct conversion between energy and velocity at such low energies, which makes a comparison very uncertain.

From Fig. 11 we see that the 2D losses occur only for small energies, at 5 eV the bulk losses take over. The 2D losses go to zero quite slowly, just like the bulk losses, but on another energy scale. If we only had 2D losses, the minimum mean free path would be long, about 20 Å. The general behavior of the 3D mean free path follows a well known pattern. The mean free path has a minimum of about 5 Å at an energy of 3-4 times the energy where the loss function has its center of gravity. We have used the Born approximation to evaluate the mean free paths. This may seem a very crude approximation at low energies. However the Born scattering expression with a basis of Bloch waves and Bloch energies rather than plane waves and free electron energies agrees with the GW approximation, which is commonly used also at low energies. Further it was shown by Campillo et al [73] that plane waves and free electron energies was not that bad, as long as the energies in the dielectric function are well approximated.

Our main concern is the behavior of the effective broadening function at small energies where it is dominated by the 2D losses. The 3D contributions set in at somewhat higher energies, and give a rather structureless contribution. What we here for convenience call 2D losses is of course actually also a 3D effect since it comes from excitations of a coupled set of 2D layers. To allow a qualitative discussion we represent the  $\alpha_{2D}$  functions by a rectangular distribution. The rectangular distribution allows an analytic solution valid out to the cut-off  $\omega_0$  ( $\omega_0 \simeq 0.08$  au  $\simeq 2.2$  eV).  $P_{\mathbf{k}}(\omega)$  has only a fairly small tail beyond  $\omega_0$ . In Fig. 12 we plot the total  $P_{\mathbf{k}}(\omega)$  function (sum over the four first layers, properly mean free path weighted), calculated with the rectangular approximation and broadened with Lorentzians of different widths. We note the marked asymmetry. If the  $J_{2D}$  function has a power law singularity with singularity index  $\alpha_L$ , the photoemission will have a singularity index



$(\alpha_0 + \alpha_L)$ .

In a paper by Liu, Anderson and Allen from 1991 [74], they discussed the lineshapes of  $Bi_2Sr_2BaCu_2O_8$  along the  $\Gamma - X$  direction obtained by Olsen et al [75] for 22 eV photons. They concluded that neither the Fermi liquid nor the marginal Fermi liquid theories could fit the slow fall-off of the spectrum at higher energies. Our results offer a possibility that the slow falloff may be due to intrinsic creation of acoustic plasmons in a coupled set of  $CuO$  layers, an effect not present if only one  $CuO$  layer is considered. This broadening is mostly intrinsic, i.e. if we treat a 3D system we have an almost intrinsic effect. However most theoretical discussions concern an isolated 2D system, compared to which we find an appreciable extra broadening from the coupling between the layers.

The PES spectra change strongly when we go to the superconducting state. The main peak sharpens and a peak-dip-hump structure develops. This effect has been interpreted as a coupling of the 2D state to the  $(\pi, \pi)$  collective mode. [62] Here we find that this effect also can arise from the gapping of the loss function caused by the lack of low energy excitations in a superconductor as shown in Fig. 13. Without a more accurate model we find it difficult to decide which is the correct explanation, possibly it could be a combination of both mechanisms. Since the gapping of the loss function is related to the superconducting gap, also with our mechanism the hump will scale with the gap. It is clear that the experimental peak-dip-hump structure rides on a background which is not predicted by our expressions, nor by anyone else's. Our theory is however rather schematic with its strict separation of a 2D and a 3D part, while in reality the bands are hybridized. If we extend our approach to a more detailed treatment of the underlying bandstructure, the background could well be strongly changed. Such an extension represents a very large numerical task, but with the present pilot treatment we can at least start thinking seriously about the difficult background problems in photoemission.

In a recent paper Haslinger and Joynt [58] discussed a broadening mechanism due to the interaction between the photoelectron when outside the solid and the electrons in the solid. This is a different mechanism than in this paper, which adds additional broadening. This mechanism has also been discussed by Schulte et. al. [76]

It should be stressed that we cannot claim any high quantitative accuracy. We have put in dispersion in the loss function using a crude approximation. Since however dispersion is very important we think our predictions are substantially better than if dispersion had been neglected. We have only considered normal emission where the electrons come from the  $\Gamma$  point, while the interesting experiments concern electrons from the Fermi surface. However there is no reason that the effective loss function should change qualitatively when we go away from normal emission. The behavior of the loss function when  $\omega \rightarrow 0$  has been disputed. Most authors seem to believe the approach is linear, but there are also claims that it

should be quadratic. [77] If it were quadratic, the corresponding  $\alpha$ -function would start linearly rather than with a constant. However  $\alpha(\omega)$  would have to rise very fast to reproduce the behavior of the loss function for the (quite small) energies where it is known to be approximately linear. Thus the pure power law behavior of  $P_k(\omega)$  would be lost, but Lorentzian broadened curves would probably not differ much. Our fluctuation potentials are obtained by phase-shifting bulk potentials to make them zero at the surface, and define them as zero outside the solid. This procedure turned out to be fairly good in the metallic case, where we could check with more accurately calculated fluctuation potentials. Again this approximation is crude, but we believe it to be fundamentally better than if we had used a step function on the bulk potential. Since the phase of the bulk potential is arbitrary, such a procedure would anyhow have been arbitrary. To calculate more accurate potentials is a very large numerical undertaking.

One may also question the use of a bulk expression to estimate of the mean free path at the fairly low energies that we are concerned with, after all we found strong effects when modifying the fluctuation potentials for surface effects. It is not easy to make a strong statement here, and we can only refer to "the state of the art", that bulk mean free paths are successfully used in LEED and also in low energy life time calculations which are compared with time-resolved two-photon PES (TR-2PPE) experiments. [78]

Acknowledgement - We thank J.W. Allen, J.C. Cam-puzano, A. Fujimori, A.J. Millis, M.R. Norman, and Z.-X. Shen for constructive and informative comments. One of the authors (J. D. L.) acknowledges the fellowship from the Japan Society for the Promotion of Science.

## VII. APPENDIX A

The quasi-boson parameters are related to the dynamically screened potential  $W(\mathbf{r}, \mathbf{r}'; \omega)$ . Using its spectral resolution we can write  $W$  in terms of the fluctuation potentials  $V^q$ ,

$$\begin{aligned} W(\mathbf{r}, \mathbf{r}'; \omega) &= \int \frac{\varepsilon^{-1}(\mathbf{r}, \mathbf{r}''; \omega)}{|\mathbf{r}'' - \mathbf{r}'|} d\mathbf{r}'' \\ &= \frac{1}{|\mathbf{r} - \mathbf{r}'|} + \sum_q \frac{2\omega_q V^q(\mathbf{r}) V^q(\mathbf{r}')}{\omega^2 - \omega_q^2}, \end{aligned} \quad (36)$$

where,

$$V^q(\mathbf{r}) = \int \frac{\rho^q(\mathbf{r}') d\mathbf{r}'}{|\mathbf{r} - \mathbf{r}'|}, \quad \rho^q(\mathbf{r}) = \langle N, q | \rho_{op}(\mathbf{r}) | N \rangle, \quad (37)$$

$$\rho_{op}(\mathbf{r}) = \int \psi^\dagger(x) \psi(x) d\xi, \quad \omega_q = E(N, q) - E(N, 0) - i\delta,$$

and  $x$  stands for three space coordinates  $\mathbf{r}$ , and  $\xi$  for a spin coordinate. Since  $\omega_q$  and  $V^q$  are not known exactly we use the RPA where

$$V^q(\mathbf{r}) = \int W(\mathbf{r}, \mathbf{r}'; \omega_q) \tilde{\phi}_q(\mathbf{r}') d\mathbf{r}', \quad (38)$$

with  $\omega_q = \varepsilon_k - \varepsilon_l$  ( $\varepsilon_k > \mu > \varepsilon_l$ ) and  $\tilde{\phi}_q(\mathbf{r}) = \phi_k(\mathbf{r}) \phi_l(\mathbf{r})$ , i.e. the state  $q$  corresponds to a particle-hole excitation. Undamped plasmons represent a singular case, which requires a special treatment. [21], [22] In our treatment we will take the state "q" as a quasi-boson state. In our applications to photoemission the fluctuation potentials  $V^q$  always appear in a quadratic form together with  $\omega_q$  such that they can be eliminated and replaced with the imaginary part of the screened potential  $\text{Im} W$

$$\text{Im} W(\mathbf{r}, \mathbf{r}'; \omega) = -\pi \sum_q V^q(\mathbf{r}) V^q(\mathbf{r}') \delta(\omega - \omega_q), \quad \omega > 0. \quad (39)$$

$\text{Im} W$  in turn can be estimated from experimental electron energy loss data.

## VIII. APPENDIX B

To find the ground state for the Hamiltonian in Eq. 12 we replace  $c_l^\dagger c_{l'}$  by  $\delta_{ll'} - c_{l'} c_l^\dagger$  to have

$$H_{\text{sys}} = \sum_l \varepsilon_l c_l^\dagger c_l + \sum_q \omega_q a_q^\dagger a_q - \sum_{ql'} V_{ll'}^q c_{l'} c_l^\dagger [a_q + a_q^\dagger] + \sum_{ql} V_{ll}^q [a_q + a_q^\dagger]. \quad (40)$$

The last term can be combined with the quadratic boson term, and the linear boson operator eliminated by a shift,

$$a_q = \tilde{a}_q - \frac{V_0^q}{\omega_q}, \quad V_0^q = \sum_l V_{ll}^q,$$

to obtain

$$H_{\text{sys}} = \sum_l \varepsilon_l c_l^\dagger c_l + \sum_q \omega_q \tilde{a}_q^\dagger \tilde{a}_q - \sum_{ql'} V_{ll'}^q c_{l'} c_l^\dagger \left[ \tilde{a}_q + \tilde{a}_q^\dagger - 2 \frac{V_0^q}{\omega_q} \right] - \sum_q \frac{(V_0^q)^2}{\omega_q} \quad (41)$$

The last term in the square bracket is combined with the first term, which then is diagonalized. This gives

$$H_{\text{sys}} = \sum_l \tilde{\varepsilon}_l \tilde{c}_l^\dagger \tilde{c}_l + \sum_q \omega_q \tilde{a}_q^\dagger \tilde{a}_q - \sum_{ql'} \tilde{V}_{ll'}^q \tilde{c}_{l'} \tilde{c}_l^\dagger [\tilde{a}_q + \tilde{a}_q^\dagger] + \sum_q \frac{(V_0^q)^2}{\omega_q}.$$

The ground state for  $H_{\text{sys}}$  is thus a filled Fermi sea with no quasi-bosons  $\tilde{a}_q$ , i.e. a simple Slaterdeterminant  $|N^{IP}\rangle$ , and its energy is  $E_0 = \sum_l \tilde{\varepsilon}_l + \sum_q (V_0^q)^2 / \omega_q$ . This is also the ground state for  $H$  since it does not contain any photoelectron and thus both  $h$  and  $V$  give zero. The transformation matrix that diagonalizes the  $c_l^\dagger c_l$  term deviates from  $\delta_{ll'}$  by terms of order  $(V^q)^2$ , and we will neglect the difference between  $\tilde{V}_{ll'}^q$  and  $V_{ll'}^q$  and between  $\tilde{\varepsilon}_l$  and  $\varepsilon_l$ . When the occupied state  $l$  is a core state the transformation matrix is unity and  $\tilde{V}_{ll'}^q = V_{ll'}^q$ .

The state  $c_l |N^{IP}\rangle$  appearing in Eq. 15 is not an eigenstate of  $H_{\text{sys}}$ . We note that states  $\{c_l |N^{IP}\rangle\}$ ,  $\{\tilde{a}_q^\dagger c_l |N^{IP}\rangle\}$ ,  $\{\tilde{a}_q^\dagger \tilde{a}_{q'}^\dagger c_l |N^{IP}\rangle\}$  form a complete set to span  $|N-1, s\rangle$ . We have to lowest order in the coupling functions  $V^q$

$$|l\rangle = |l\rangle^0 + \sum_{ql'} \frac{V_{ll'}^q}{\omega_q - \varepsilon_{l'} + \varepsilon_l} |ql'\rangle^0$$

where

$$|l\rangle^0 = c_l |N^{IP}\rangle, \quad |ql\rangle^0 = \tilde{a}_q^\dagger c_l |N^{IP}\rangle,$$

We express the "initial state"  $|l\rangle^0$  in eigenstates of  $H_{\text{sys}}$ ,

$$|l\rangle^0 = |l\rangle - \sum_{ql'} \frac{V_{ll'}^q}{\omega_q - \varepsilon_{l'} + \varepsilon_l} |ql'\rangle.$$

We need the matrix elements  $T_s$  (c.f. Eq. 15),

$$T_s = \left\langle N-1, s \left| \left( 1 + V \frac{1}{E - H_{\text{sys}} - h - QVQ} \right) c_{l'} \right| N^{IP} \right\rangle.$$

We are interested in the two cases when "s" corresponds to  $|l\rangle$  and to  $|ql\rangle$ ,

$$\begin{cases} |N-1, s\rangle = |l\rangle \\ E(N-1, s) = E(N) - \varepsilon_l \end{cases},$$

$$\begin{cases} |N-1, s\rangle = |ql\rangle \\ E(N-1, s) = E(N) - \varepsilon_l + \omega_q \end{cases}.$$

We have, neglecting  $O(V^2)$  terms,

$$T_l = \left\langle l \left| \left( 1 + V \frac{1}{E - H_{\text{sys}} - h - QVQ} \right) \right| l' \right\rangle^0 = \delta_{ll'}$$

$$\begin{aligned} T_{ql} &= \left\langle ql \left| \left( 1 + V \frac{1}{E - H_{\text{sys}} - h - QVQ} \right) \right| l' \right\rangle^0 \\ &= \frac{-V_{l'l}^q}{\omega_q - \varepsilon_l + \varepsilon_{l'}} + \delta_{ll'} V^q \frac{1}{\omega_q + \varepsilon_{\mathbf{k}} - h - \Sigma(\omega_q + \varepsilon_{\mathbf{k}})}. \end{aligned}$$

Combining these results with Eqs.1 and 15 we have,

$$J_{\mathbf{k}}(\omega) = \sum_l |\tau_l(\mathbf{k})|^2 \delta(\omega - \varepsilon_{\mathbf{k}} + \varepsilon_l) \quad (42)$$

$$+ \sum_{ql} |\tau_{ql}(\mathbf{k})|^2 \delta(\omega - \omega_q - \varepsilon_{\mathbf{k}} + \varepsilon_l)$$

with

$$\tau_l(\mathbf{k}) = \langle \tilde{\mathbf{k}} | \Delta | l \rangle$$

$$\tau_{ql}(\mathbf{k}) = \sum_{l'} \frac{-\langle \tilde{\mathbf{k}} | \Delta | l' \rangle V_{l'l}^q}{\omega_q - \varepsilon_l + \varepsilon_{l'}} \quad (43)$$

$$+ \left\langle \tilde{\mathbf{k}} \left| V^q \frac{1}{\omega_q + \varepsilon_{\mathbf{k}} - \hbar - \Sigma(\omega_q + \varepsilon_{\mathbf{k}})} \Delta \right| l \right\rangle.$$

Here the first term is the intrinsic and the second the extrinsic amplitude. For photoemission from a core level only one state is involved, and we can replace all  $l$  by one single index, say  $c$ . Our expression then reduces to our earlier result in Refs. [20] and [21]. Since  $\tau_{ql}(\mathbf{k})$  is quadratic in the fluctuation potentials  $V^q$  Eq. 43 can also be written in terms of  $\text{Im} W$ .

## IX. REFERENCES

- 
- [1] O.K. Andersen, T. Saha-Dasgupta, R.W. Tank, C. Arcangeli, O. Jepsen, and G. Krier in *Electronic Structure and Physical Properties of Solids, Lect. Notes in Phys., vol. 535*, ed. by H. Dreyssé, p. 3 (2000). Springer, Berlin
- [2] F. Aryasetiawan and O. Gunnarsson, Phys. Rev. B **49**, 7219 (1994)
- [3] J. D. Lee, O. Gunnarsson, and L. Hedin, Phys. Rev. B **60**, 8034 (1999)
- [4] L. Hedin and J. D. Lee, Phys. Rev. B **64**, 115109 (2001)
- [5] J. B. Pendry, Surface Science **57**, 679 (1976)
- [6] J. B. Pendry in *Photoemission and the electronic properties of surfaces*, ed. by B. Feuerbacher, B. Fitton, and R. F. Willis, p. 87 (1978). Wiley, New York
- [7] J. E. Inglesfield and E. W. Plummer in *Angle-resolved photoemission*, ed. by S. D. Kevan, Elsevier, Amsterdam 1992
- [8] W. Schattke, Progr. Surf. Sci. **54**, 211 (1997)
- [9] O. Gunnarsson, K. Schönhammer, J. W. Allen, K. Karlsson, and O. Jepsen, J. Electron Spectrosc. Relat. Phenom. **117-118**, 1 (2001)
- [10] S. D. Kevan and Eli Rotenberg, J. Electron Spectrosc. Relat. Phenom. **117-118**, 57 (2001)
- [11] D. Claesson, S.-A. Lindgren, L. Wallden, and T.-C. Chiang, Phys Rev Lett **82**, 1740 (1999)
- [12] C. Caroli, D. Lederer-Rosenblatt, B. Roulet and D. Saint-James, Phys. Rev. B **8**, 4552 (1973)
- [13] W. I. Schaich and N.W. Ashcroft, Phys. Rev. B **3**, 2452 (1971)
- [14] L. V. Keldysh, Sov. Phys.-JETP **20**, 1018 (1965)
- [15] P. J. Feibelman and D.E. Eastman, Phys. Rev. B **10**, 4932 (1974)
- [16] J. F. L. Hopkinson, J. B. Pendry and, D. J. Titterton Comp. Phys. Comm. **19**, 69 (1980)
- [17] C.-O. Almbladh, Physica Scripta **32**, 341 (1985)
- [18] M. L. Goldberger, and K.M. Watson, *Collision Theory* (Wiley, New York, 1964)
- [19] The states above the vacuum level have free electron energies since in photoemission the normalization volume is always much larger than the volume of the solid (which in turn tends to infinity). The matrix elements in the photoemission expression however make the quasiparticle energies enter.
- [20] W. Bardyszewski and L. Hedin, Physica Scripta **32**, 439 (1985)
- [21] L. Hedin, J. Michiels, J. Inglesfield, Phys. Rev. B **58**, 15565 (1998)
- [22] L. Hedin, J. Phys.: Condens. Matter **11**, R489 (1999)
- [23] G. D. Mahan, *Many-Particle-Physics* (Plenum, New York, 1981)
- [24] P. H. Citrin, G. K. Wertheim, and Y. Baer, Phys. Rev. B **16**, 4256 (1977)
- [25] D. J. Spanjaard, D. W. Jepsen, and P. M. Marcus, Phys Rev B **15**, 1728 (1977)
- [26] G. D. Mahan, Phys Rev B **2**, 4334 (1970)
- [27] T. Miller and T.-C. Chiang, J. Electron Spectrosc. Relat. Phenom. **117-118**, 413 (2001)
- [28] S. Hüfner, R. Claessen, F. Reinert, Th. Straub, V. N. Strocov, and P. Steiner, J. Electron Spectrosc. Relat. Phenom. **100**, 191 (1999)
- [29] N. V. Smith, P. Thiry, Y. Petroff, Phys Rev B **47**, 15476 (1993)
- [30] See e. g. V. N. Strocov, P. Blaha, H. I. Starnberg, M. Rohlfiing, R. Claessen, J.-M. Debever, and J.-M. Themlin, Phys Rev B **61**, 4994 (2000)
- [31] C. N. Berglund and W.E. Spicer, Phys. Rev. **136**, A1030 (1964)
- [32] The classic paper here is S. Tougaard and P. Sigmund, Phys. Rev. B **25**, 4452 (1982). A fairly recent paper estimating the important effects of elastic scattering is I. S. Tilinin, A. Jablonski and S. Tougaard, Phys. Rev. B. **52**, 5935 (1995)
- [33] H. Höchst, P. Steiner, and S. Hüfner, J. Phys. F: Metal Phys. **7**, L309 (1977)
- [34] P. Steiner, H. Höchst, and S. Hüfner, in *Photoemission in Solids II*, eds L. Ley and M. Cardona, Springer 1979
- [35] S. Hüfner, *Photoelectron Spectroscopy*, Springer 1995
- [36] D. R. Penn, Phys Rev Lett **40**, 568 (1978)
- [37] F. Aryasetiawan, L. Hedin, K. Karlsson, Phys. Rev. Lett. **77**, 2268 (1996)
- [38] W. J. Pardee, G. D. Mahan, D. E. Eastman, R. A. Pollak, L. Ley, F. R. McFeely, S. P. Kowalczyk, and D. A. Shirley, Phys. Rev. B **11**, 3614 (1975)
- [39] D. R. Penn, Phys. Rev. Lett. **38**, 1429 (1977)
- [40] D. C. Langreth, Phys. Rev. B **1**, 471 (1970)
- [41] J. J. Chang and D.C. Langreth, Phys. Rev. B **5**, 3512 (1972)

- [42] J. J. Chang and D.C. Langreth, Phys. Rev. B **8**, 4638 (1973)
- [43] J. Inglesfield, Solid State Commun. **40**, 467 (1981)
- [44] J. Inglesfield, J. Phys. C **16**, 403 (1983)
- [45] S. A. Flodström, R. Z. Bachrach, R. S. Bauer, J. C. McMenamin, and S. B. M. Hagström, J. Vac. Science and Techn. **14**, 303 (1977)
- [46] L. Hedin, Physica Scripta **21**, 477 (1980)
- [47] T. Fujikawa and L. Hedin, Phys Rev B **40**, 11507 (1989)
- [48] L. Hedin, Phys Rev **139**, A796, (1965)
- [49] R. H. Ritchie and A. Howie, Philos. Mag. **36**, 463 (1977)
- [50] S. Tougaard and B. Jörgensen, Surf. Sci. **143**, 482 (1984)
- [51] T. A. Carlson and M. O. Krause, Phys. Rev. **140**, A1057 (1965)
- [52] J. Stöhr, R. Jaeger, and J. J. Rehr, Phys. Rev. Lett. **51**, 821 (1983)
- [53] D. A. Shirley, U. Becker, P. A. Heimann, and B. Langer, J. de Physique, Colloque C9, vol **48**, C9-427 (1987)
- [54] U. Becker and D. A. Shirley, Physica Scripta **T31**, 56 (1990)
- [55] T. D. Thomas, Phys. Rev. Lett. **52**, 417 (1984)
- [56] C.-O. Almbladh and L. Hedin, p 607 in *Handbook on synchr. rad. vol 1* (ed E E Koch, North Holland, 1983)
- [57] C. J. Tung, and R. H. Ritchie, Phys. Rev. B **16**, 4302 (1977)
- [58] R. Haslinger and R. Joynt, J. Electron Spectrosc. Relat. Phenom. **117-118**, 31 (2001)
- [59] M. R. Norman, M. Randeria, H. Ding, and J. C. Campuzano, Phys. Rev. B **59**, 11191 (1999)
- [60] N. Nücker, H. Romberg, S. Nakai, B. Scheerer, J. Fink, Y. F. Yan, and Z. X. Zhao, Phys. Rev. B **39**, 12379 (1989)
- [61] S. Doniach and M.J. Sunjic, J. Phys. C **3**, 28 (1970)
- [62] J.C. Campuzano, H. Ding, M. R. Norman, H.M. Fretwell, M. Randeria, A. Kaminski, J. Mesot, T. Takeuchi, T. Sato, T. Yokoya, T. Takahashi, T. Moshiku, K. Kadowaki, P. Guptasarma, D.G. Hinks, Z. Konstantinovic, Z.Z. Li, and H. Raffy, Phys. Rev. Lett. **83**, 3709 (1999)
- [63] We are indebted to Drs Z. X. Shen and A. Yurgens for providing informative viewpoints and unpublished background data.
- [64] A. Yurgens, T. Claeson, S.-J. Hwang, and J.-H. Choy, Int. J. Mod. Phys. B **13**, 3758 (1999), and paper presented at the APS meeting Seattle 2001
- [65] J. R. Schrieffer, D. J. Scalapino, and J. W. Wilkins, Phys. Rev. Lett. **10**, 336 (1963)
- [66] C.-O. Almbladh, Phys. Rev. B **16**, 4343 (1977)
- [67] J.Zaanan and G.A.Sawatzky, Phys. Rev. B **33**, 8074 (1986)
- [68] A.W.Kay, F.J.Garcia de Abajo, S.-H.Yang, E.Arenholz, B.S.Mun, N.Mannella, Z.Hussain, M.A.Van Hove, and C.S.Fadley, Phys. Rev. B **63**, 115119 (2001)
- [69] A. Kotani, J. Electron Spectrosc. Relat. Phenom. **100**, 75 (1999)
- [70] J. W. Gadzuk, J. Electron Spectrosc. **11**, 355 (1977)
- [71] T. Takahashi, H. Matsuyama, H. Katayama-Yoshida, Y. Okabe, S. Hosoya, K. Seki, H. Fujimoto, M. Sato, and H. Inokuchi, Phys. Rev. B **39**, 6636 (1989)
- [72] W. Nessler, S. Ogawa, H. Nagano, H. Petek, J. Shimoyama, Y. Nakayama, and K. Kishio, Phys. Rev. Lett. **81**, 4480 (1998)
- [73] I. Campillo, J. M. Pitarke, A. Rubio, E. Zarate, and P. M. Echenique, Phys. Rev. Lett. **83**, 2230 (1999)
- [74] L. Z. Liu, R. O. Anderson, and J. W. Allen, J. Phys. Chem. Solids **52**, 1473 (1991)
- [75] C. G. Olson et al, Phys. Rev. B **42**, 381 (1990)
- [76] K. Schulte, M.A.James, P.G.Steeneken, G.A.Sawatzky, R.Suryanarayanan, G.Dhalenne, and A.Revcolevschi, Phys. Rev. B **63**, 165429 (2001)
- [77] I. Bozovic, Phys. Rev. B **42**, 1969 (1990)
- [78] P. M. Echenique, J. M. Pitarke, E. V. Chulkov, and A. Rubio, Chemical Physics **251**, 1 (2000)